DTU Library

Thermodynamic analysis of polygeneration systems based on catalytic hydropyrolysis for the production of bio-oil and fuels

Nguyen, Tuong-Van; Clausen, Lasse Røngaard

Published in:
Energy Conversion and Management

Link to article, DOI:
10.1016/j.enconman.2018.06.024

Publication date:
2018

Document Version
Peer reviewed version

Citation (APA):
Nguyen, T-V., & Clausen, L. R. (2018). Thermodynamic analysis of polygeneration systems based on catalytic hydropyrolysis for the production of bio-oil and fuels. *Energy Conversion and Management*, *171*, 1617-1638. https://doi.org/10.1016/j.enconman.2018.06.024

Thermodynamic analysis of polygeneration systems based on catalytic hydropyrolysis for the production of bio-oil and fuels

Tuong-Van Nguyen[a,*], Lasse Røngaard Clausen[a]

[a]*Section of Thermal Energy, Department of Mechanical Engineering, Technical University of Denmark, Building 403, Nils Koppels Allé, 2800 Kongens Lyngby, Denmark*

Abstract

Novel polygeneration concepts based on catalytic hydropyrolysis and hydrodeoxygenation are presented and compared via process simulation and thermodynamic analysis. These systems process and convert biomass into high-quality bio-oil and fuels such as synthetic natural gas (SNG), molecular hydrogen (H_2) and methanol (MeOH). Twelve system layouts were evaluated and compared with regards to their energy demands and performances. Detailed thermodynamic models were developed, considering the different technological alternatives for the valorisation of bio-char, removal of carbon dioxide, fuel upgrading and water electrolysis, as well as the opportunities for energy integration. The results show that the standard system, which produces only bio-oil, reaches an energy efficiency of 61 % (LHV). This value can be increased by 7 to 28 %-points when co-producing SNG, 10 to 21 %-points when producing H_2, and 10 to 19 %-points when producing MeOH. The highest values are achieved by co-production of SNG as light hydrocarbons are produced in the hydropyrolysis, and limited processing is therefore required to reach the desired product quality. High system efficiencies are possible mainly because of the high efficiency of the core hydropyrolysis process. Carbon conversion efficiencies are highest when generating SNG or MeOH and reach a maximum when electrolysis and char gasification are implemented (98 % and 95 %). The performance of these polygeneration systems is strongly impacted by the type of CO_2-separation process and electrolyser - these processes have a strong influence on the power and heating demands, as well as on the potential energy savings and waste heat valorisation.

Keywords: Biomass, green fuels, hydropyrolysis, hydrodeoxygenation

1. Introduction

The Danish transport sector emitted about 13.2 mill. tonnes CO_2-equivalent in 2010, of which 92 % was attributable to road transport (e.g. passenger cars and vans) [1]. The emissions were overall stable since, but are expected to increase in the near-future because of increasing road activity. In this context, the

*Principal corresponding author. Tel.: +45 4525 4129
Email addresses: tungu@mek.dtu.dk (Tuong-Van Nguyen), lrc@mek.dtu.dk (Lasse Røngaard Clausen)

Nomenclature

$\dot{Q}$	Heat rate, W
$\dot{W}$	Power, W
$\dot{m}$	Mass flowrate, kg/s
$\tilde{c}$	Molar fraction, mol/mol
x	Mass fraction, kg/kg
T	Temperature, K or °C
p	Pressure, Pa
Abbreviations	
AEC	Alkaline Electrolyser Cell
DEPG	Dimethyl Ether of Polyethylene Glycol
DNA	Dynamic Networks Analysis
EOS	Equation of State
HDO	Hydrodeoxygenation
LHV	Lower Heating Value
MEA	Monoethanolamine
MeOH	Methanol
NRTL	Non-Random Two-Liquids
PC	Perturbated Chain
PSA	Pressure Swing Adsorption
SAFT	Statistical Associating Fluid Theory
SN	Stoichiometric Number
SNG	Synthetic Natural Gas
SOEC	Solid Oxide Electrolyser Cell
WGS	Water Gas Shift
Greek letters	
Δh^0	Lower heating value, J/kg
Δh_r^0	Standard enthalpy of reaction, J/mol
η	energy efficiency
Subscripts	
system	system
total	total

recent Danish governments had set out a strategy on clean and energy-efficient vehicles. A main goal is to substitute transportation fuels derived from petroleum with ones derived from biomass.

Biomass can be converted into high-value chemicals, fuels, power and heat by undergoing thermal, chemical or biological processing and separation. Several studies in the scientific literature deal with the modelling and optimization of pathways from biomass to transportation fuels. For example, Baliban et al.[2] focused on the conversion of hardwood biomass to gasoline, diesel and jet fuel, analysing the Fischer-Tropsch and methanol synthesis pathways. Niziolek et al.[3] performed a similar analysis, analysing the production routes from coal and two types of biomass, optimizing the system topology to minimize the costs. Onel et al.[4] reviewed the work on biomass/coal refineries for fuel production, and discussed the advances in this field. They argued that polygeneration systems result in lower production costs, and increase the competitivity of biomass-derived fuels.

Pyrolysis is a thermal process for converting biomass into a liquid product that can be further upgraded into a transportation fuel. It is defined as the thermal decomposition in an oxygen-free environment by heating from approximately 250 to 650 °C. It releases volatile gases, of which a part condenses into a viscous fluid named bio-oil, as well as solids collected as char. The operating conditions (temperature, pressure, heating rate and residence time) have a direct effect on the yield and composition of each product. Flash pyrolysis, i.e. pyrolysis with heating rate of up to $10^4\,\mathrm{K{\cdot}s^{-1}}$, results in higher liquid yield than slow pyrolysis [5].

The produced bio-oil has undesirable properties: high oxygen and water contents, low heating value, high acidity, high viscosity, non-miscibility with conventional fossil fuels, and short shelf life. Upgrading is necessary to reduce the oxygen content, stabilise the bio-oil and produce a diesel- or gasoline-like fuel. Catalysts are necessary, but their lifetimes are short because of carbon deposition and sulphur poisoning. A promising route is to combine pyrolysis [6] and hydrodeoxygenation (HDO) in a catalytic hydropyrolysis process [7]. When performing these reactions in a hydrogen-rich environment at high pressure [8], oxygen atoms are converted into water, carbon oxides and hydrocarbons before condensation of the bio-oil. Parasite reactions such as polymerization and coking are then avoided, leading to a high-grade oil product [9].

The present work focuses on catalytic hydropyrolysis coupled with deep hydrodeoxygenation in a second reactor (sometimes referred as ex-situ hydrotreating [8]). Fast hydropyrolysis is carried out in a catalytic reactor and the produced vapours undergo upgrading in a second unit, usually a catalytic packed bed. An advantage of having two separate reactors is a better system control and optimization, as the reactors can operate in different conditions. Venkatakrishnan et al.[10] at Purdue University developed the H2Bioil system, in which fast hydropyrolysis takes place at 480-580 °C and the produced vapours undergo hydrodeoxygenation reactions in a catalytic bed at 300-375 °C. Experimental studies in parallel [11] show how the catalyst selection impacts strongly the distribution of hydrocarbons in the liquid yield. GTI developed the IH2 system, in which fast hydropyrolysis also takes place in presence of a catalyst. Similar temperature and pressure ranges as in Venkatakrishnan et al.[10] are reported, and tests were performed to validate the proposed concept.

These systems are further detailed in the Purdue [12] and GTI [13] patents. The former suggests the use of a carbon-free energy source, such as solar energy, to generate hydrogen, heat or electricity to convert biomass into bio-oil, which is then further upgraded. Synergies with thermo-chyemical and biological processes are discussed to extend the product portfolio to other liquid fuels such as alcohols. The latter focuses specifically on the hydropyrolysis and hydroconversion route, aiming to develop a self-sustaining process for liquid fuel production. According to the authors, the economics of such systems depend mainly on the hydrogen and feedstock prices, as well as on the system capital cost and selling price of the liquid product. Marker et al.[14] demonstrate the proof-of-concept of their integrated hydropyrolysis and hydroconversion (IH2) system for the direct production of bio-oil, using experimental data a pilot plant operating on a feed flowrate of 0.45 kg/h in semi-continuous conditions. In a further work, they present the experimental data from the pilot plant, operating on 50 kg/day, on a continuous basis (750 h). Tan et al.[15] performed a techno-economic analysis of the standard GTI system. They estimated a total capital investment of M$ 264 for a processing capacity of 2000 dry metric tonnes of woody biomass per day and found that the hydrogen plant, followed by the hydropyrolysis section, represented the biggest share of the capital costs. Stummann et al.[16] performed an experimental investigation using beach wood, and analysed how changes in temperature (365-511 °C) and hydrogen pressure (1.6-3.6 MPa) impact the product yield and organic composition. Their results suggest that catalytic hydropyrolysis may be a viable biomass-to-liquid fuels pathway.

The few works in this field suggest that the main challenges are to (i) demonstrate and optimize this combined hydropyrolysis/hydrodeoxygenation process, (ii) develop the proper catalyst formulations and address the possible deactivation by carbon deposition, contamination, and mechanical break-down, (iii) and improve the system economics, depending on the system scale and hydrogen source. The present paper aims at addressing some of these gaps: it presents the conceptual design and thermodynamic analysis of biorefineries based on catalytic hydropyrolysis and hydrodeoxygenation. The presented concepts are all characterised by the production of a high-grade bio-oil, together with added-value chemicals such as synthetic natural gas, hydrogen and methanol. The impact of various layouts, operating conditions and hydrogen source on the system performance is analysed in details. The novelty of this work lies in the systematic analysis of polygeneration systems based on hydropyrolysis and hydrodeoxygenation, using process modelling tools and advanced thermodynamic methods. It investigates the opportunities for producing other chemical fuels such as synthetic natural gas, and how the system layouts actually change. Such systems were not assessed before, and only the standard IH2 system was analysed from a technical and economic perspective.

2. Methods

2.1. System design

The present paper investigates the performance of a polygeneration system (Figure 1) producing bio-oil and by-products such as synthetic natural gas (SNG), hydrogen (H_2) and methanol (CH_3OH/MeOH). Each system layout presents different characteristics with regards to the electricity and heating demand and production, generation of bio-oil, hydrogen, chemicals and char.

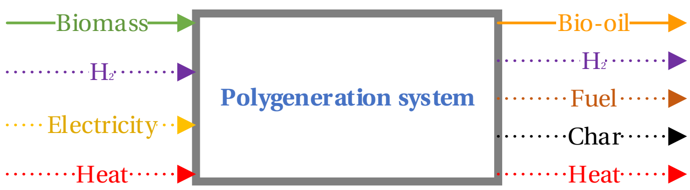

Figure 1: Schematics of the investigated polygeneration system for production of bio-oil and other green fuels through hydropyrolysis and hydrodeoxygenation.

Pressurised catalytic hydropyrolysis and hydrodeoxygenation has attracted interest because of the high quality of the produced bio-oil and the potentially high efficiency. The following steps are essential: (1) the feedstock preparation, with pressurisation, (2) the hydropyrolysis and hydrodeoxigenation, and (3) the gas-liquids separation. Biomass is fed into a pressurised and catalyst-enhanced fast hydropyrolysis reactor in the presence of hydrogen. The reactor is preferably a fluidized bed with hydrogen as fluidising agent, since biomass should be decomposed under high heating rates with short vapour residence times. Solids are removed, and the produced vapours are upgraded in a second reaction step. It takes place in another catalytic stage and at similar pressure levels. Coupling with hydrodeoxygenation results in a low oxygen content, and the production of hydrocarbons with properties in the boiling ranges of gasoline and diesel. Four phases are generated and then separated for further upgrading: (i) an organic phase composed of hydrocarbons (C_4^+), which is the target product, (ii) an aqueous phase, (iii) a solid phase, with char and ash, and (iv) a gaseous mixture consisting of hydrocarbon gases (C_1-C_3), carbon monoxide and dioxide (CO and CO_2), hydrogen and water vapour. The produced hydrocarbons are not soluble in water as conventional pyrolysis oil, meaning that the two liquid phases are easily separable into a near carbon-free water and gasoline/diesel fractions.

2.2. Process superstructure

Alternative layouts can be designed building on this process concept. The first option, presented in the Gas Technology Institute (GTI) patent [13], is to ensure that the overall polygeneration system is self-sustaining, i.e. does not require any external input other than biomass. The second option is to implement other process units to maximise the gas-liquid yield by valorising the bio-char generated in the hydropyrolysis process. The third possibility is to co-produce fuels such as SNG or MeOH. All the possible process pathways, as well as the different technological options of each step, are assembled and summarised in a process superstructure (Figure 2).

2.3. Process technologies

2.3.1. Hydrogen production

Hydrodeoxygenation is a hydrogenolysis process requiring molecular hydrogen to convert the oxygen present in the biomass feedstock into water, avoiding the production of an oxygen-rich bio-oil. It may be produced internally, through conversion of the non-condensable gases, or externally, through water or steam electrolysis. In the first case, the main steps are: gas cleaning, steam methane reforming, water-gas shift and CO_2-removal. As the non-condensable gasses mainly contain hydrogen, it is beneficial to use a pressure swing adsorption (PSA) unit. It generates a hydrogen-rich stream that can be be fed into the hydropyrolysis section, by-passing the reforming and water-gas-shift reactors. PSA processes are mature technologies widely used in the petrochemical industry for producing a hydrogen-rich product stream with a purity exceeding 98 % for a recovery of 70-90 %, depending on the system design, adsorbent and feed gas pressure. The separation efficiency is enhanced with higher hydrogen partial pressures. The addition of a PSA unit results in a smaller flowrate into the reforming section.

Hydrocarbon reforming is a strongly endothermic process for converting hydrocarbons such as methane, ethane and propane into hydrogen and carbon monoxide by reaction with steam. Water-gas-shift is a mildly exothermic reaction, included to increase the hydrogen fraction. This reaction generally takes place in two reactors operated at two different temperature levels to maximise the conversion of carbon monoxide and improve the reaction kinetics.

The addition of a CO_2-removal process, through chemical absorption with alkanoamines, or physical absorption with glycols, results in a hydrogen-rich flow that can be used in the hydropyrolysis. Chemical absorption processes consist of the removal of carbon dioxide by chemical reactions with amines in an absorber at low temperatures and pressures.

Physical absorption processes typically include an absorber, where the physical solvent dissolves the acid gas at high pressure, and a succession of flash tanks, with carbon dioxide flashed at decreasing pressure levels. The preferred solvent in the present work is a mixture of dimethyl ethers of polyethylene glycols (DEPG), i.e. the Selexol process [17]. Alternatives such as physical absorption with methanol, adsorption or membrane processes are not considered. The first one requires refrigeration, which is impractical in the present system. The two last require compression operations both prior and after the separation process to reach high removal performance and comply with the system requirements.

In case that hydrogen is not produced from the non-condensable gases, external generation of hydrogen can be ensured by electrolysis, either at low temperatures by converting water in alkaline electrolyte cells (AEC), or at high temperatures by converting steam in solid oxide electrolysis cells (SOEC). The use of electrolysis results in a higher fuel production, and is claimed to be an efficient and economically promising option [18]. A main advantage of high-temperature electrolysis is the higher reaction efficiency, and the heat of evaporation can be supplied as low-temperature heat instead of electricity [19,20]. On the contrary, low-temperature electrolysis results in the release of energy as waste heat, because the electricity input to the cell is larger than the enthalpy change of the electrolysis reaction [21]. At present, AECs are commercialised and mature technologies, while SOECs are available in niche markets, and require further development.

2.3.2. Char valorisation

Char is characterised by a high carbon content, and can be valorized in three manners: (1) through combustion, to produce the heat required in the polygeneration system; (2) through gasification, to increase the gas yield; (3) through soil incorporation, to improve the soil quality, increase agricultural productivity and sequestrate carbon. The first option may be preferred if hydrogen has to be produced internally, since reforming reactions are highly endothermic and require heat supply at high temperatures. However, it may

Table 1: List of chemical reactions occurring in the polygenation system - hydropyrolysis and hydrodeoxygenation reactions are not presented here, as they consist of complex reaction schemes involving several intermediate reactions; reactions involving sulphur, chlorine and other organic and inorganic components are neglected.

Process	Reaction	Chemistry	Δh_r^0 $[\frac{kJ}{mol}]$
Combustion	Oxidation	$C + O_2 \longrightarrow CO_2$	-394
	Partial oxidation	$C + 0.5O_2 \longrightarrow CO_2$	-111
	Partial oxidation	$2CO + O_2 \longrightarrow 2CO_2$	-283
Gasification	Water-gas	$C + H_2O \rightleftharpoons CO + H_2$	131
	Boudouard	$C + CO_2 \rightleftharpoons 2CO$	173
	C-methanation	$C + 2H_2 \rightleftharpoons CH_4$	-75
Reforming	CH_4-reforming	$CH_4 + H_2O \longrightarrow CO + 3H_2$	206
	C_2H_6-reforming	$C_2H_6 + 2H_2O \longrightarrow 2CO + 5H_2$	
	C_3H_8-reforming	$C_3H_8 + 3H_2O \longrightarrow 3CO + 7H_2$	
Water-gas-shift	WGS	$CO + H_2O \rightleftharpoons CO_2 + H_2$	-41
CO_2-removal	MEA	$2H_2O \rightleftharpoons H_3O^+ + OH^-$	
		$CO_2 + 2H_2O \rightleftharpoons H_3O^+ + HCO_3{}^-$	
		$HCO_3{}^- + H_2O \rightleftharpoons H_3O^+ + CO_3{}^{2-}$	
		$MEAH^+ + H_2O \rightleftharpoons MEA + H_3O^+$	
		$MEACOO^- + H_2O \rightleftharpoons MEA + HCO_3{}^-$	
	TEA	$CO_2 + R_3N + H_2O \rightleftharpoons R_3NH^+ + HCO_3{}^-$	
SNG synthesis	CO-methanation	$CO + 3H_2 \longrightarrow CH_4 + H_2O$	-206
	Sabatier	$CO_2 + 4H_2 \longrightarrow CH_4 + 2H_2O$	-164
MeOH synthesis	CO-to-MeOH	$CO + 2H_2 \rightleftharpoons CH_3OH$	-90.8
	CO_2-to-MeOH	$CO_2 + 3H_2 \rightleftharpoons CH_3OH + H_2O$	-49.2
Electrolysis	Water electrolysis	$H_2O \longrightarrow H_2 + \frac{1}{2}O_2$	237

be challenging to design an efficient combustion system that transfers most of the generated heat to the high-temperature reactor. The second option results in an increased fuel output, but requires steam and/or oxygen - the focus in this paper is on steam hydrogasification [22]. Carrying out the gasification process in a hydrogen-rich environment, without oxygen, leads to smaller CO_2-removal processes and lower equipment costs. The addition of steam leads to a higher fraction of both methane and hydrogen in the synthesis gas. The third option is not analysed further in the present work.

2.3.3. *Fuel synthesis*

Fuels such as SNG and MeOH can be generated from the produced syngas. The non-condensable gases contain a significant fraction of light hydrocarbons, implying that only the carbon oxides should be converted into methane to produce a high-quality SNG. The reactions taking place in the methanation process [23] are thermodynamically favoured at low temperatures and high pressures. Adiabatic reactors [24] are the simplest design option, since no reactor cooling is needed, and moderate amounts of catalyst are required. However, the temperature increase may cause catalyst sintering and the resulting equilibrium state is not optimal regarding the carbon oxides conversion. On the contrary, isothermal reactors allow for higher methane yield, but need continuous heat removal and high amounts of catalyst to compensate for the lower reaction rates at moderate temperatures. Methanol is synthesised by exothermal catalytic reactions, involving as well carbon oxides and hydrogen [25,26]. As for methanation, adiabatic or quasi-isothermal reactors [27] may be implemented, with the same advantages and issues regarding the conversion rate and reaction kinetics.

2.4. System layouts

All possible system layouts can be grouped into thirteen types (Table 2). B is the standard system layout, with bio-oil generation and hydrogen production from reforming of the light gases. The prefixes 'SNG', 'H2' and 'MeOH' indicate which fuel is produced in addition to bio-oil. The prefixes 'R' and 'E' denote whether the hydrogen required in the pyrolysis process is generated by reforming of the light gases or by water electrolysis. The prefixes 'C' and 'G' stand for combustion and gasification, if char is valorized.

Table 2: List of investigated configurations

Layout	Fuel	H_2-production	Char use	Upgrading	Reformer heating
B	none	Reforming	-	PSA	Gas combustion
SNG-R	SNG	Reforming	-	PSA	Electrical
SNG-R-C	SNG	Reforming	Combustion	PSA	Char combustion
SNG-R-G	SNG	Reforming	Gasification	PSA	Electrical
SNG-E	SNG	Electrolysis	-	-	-
SNG-E-G	SNG	Electrolysis	Gasification	-	-
H2-R-G	H_2	Reforming	Gasification	PSA	Electrical
MeOH-R-G	MeOH	Reforming	Gasification	PSA	Electrical
MeOH-E-G	MeOH	Electrolysis	Gasification	PSA	Electrical

These thirteen layouts can be further subdivided depending on the technologies used for performing specific process operations, such as CO_2-capture and electrolysis. In the rest of this study, the suffixes 'CA' and 'PA' indicate whether chemical or physical absorption is implemented. The suffixes 'SE' and 'AE' stand for solid oxide and alkaline electrolysis. For example, a polygeneration system with SNG production, hydrogen production by reforming and char gasification is denoted SNG-R-G. It can either be designed with a chemical absorption unit (SNG-R-G-CA) or a physical one (SNG-R-G-PA).

2.5. System modelling

The polygeneration plants were modelled using the software Dynamic Networks Analysis (DNA) [28], which is an in-house tool developed at the Technical University of Denmark for design of energy plants, and the flowsheeting software Aspen Plus, version 7.2, for simulation of the CO_2-removal processes and the methanol synthesis step. The important assumptions and design parameters used for each model are presented in the following sections. The biomass considered in the modelling process is maple wood [29], with the following ultimate analysis: 6.3 % hydrogen, 43.3 % oxygen, 0.11 % nitrogen, 49.2 % carbon and 1.1 % ash. This composition is chosen based on the experimental set-up of the IH^2 project, and the higher heating value, on a dry basis, is 20 MJ/kg.

2.5.1. Hydropyrolysis and hydrotreatment

The hydropyrolysis and hydrodeoxygenation processes are modelled as a black-box, without considering the kinetics and equilibrium of each individual reaction. The model inputs (i.e. the required information, not the actual inflows) are the biomass flowrate and composition, on an ultimate basis, and the design parameters such as the pressure and temperature. The model outputs are the hydrogen demand, yields of the gas, aqueous, liquid and solid phases, and their compositions. The model is calibrated using the experimental results of the IH^2 project, and the simulations are conducted based on experiment 5/25 (details given in Appendix A). The system pressure is about 22 bar and the hydropyrolysis and hydrodeoxygenation temperatures is approximately 430 °C. On a weight basis, the hydrogen input corresponds to about 4.6 % of the biomass feed, and the product yields are: 28 % bio-oil, 31 % light gases, 9 % char and 36 % water. On a lower heating value basis, the hydrogen input corresponds to about 29.5 % of the biomass feed, and the product yields are: 61 % bio-oil, 43 % light gases and 15 % char. These numbers are used to fix the yield and composition of each product. Perfect phase separation is assumed, meaning that neither bio-char nor bio-oil are entrained in the gas flow.

2.5.2. Gas purification

The PSA unit is represented by a black-box model and the adsorption mechanisms are not modelled in details. The model takes as inputs the feed characteristics, expected hydrogen recovery rate and purity, and the model outputs are the outflow properties and power demand associated with the compression of the purge gas. The recovery rate is assumed to be 87 % and the product purity is set to 99.99 %, by analogy with the Polybed version of the PSA process [30], which consists of 10 columns and 11 steps. The recovered hydrogen is at feed pressure, i.e. about 22 bar, while the purge gas is at a desorption process of 1.1 bar. More complex layouts, such as the ones that include recompression of the purge gas followed by a second PSA column to enhance the hydrogen recovery are not considered. Other gas upgrading processes are not modelled in details in the present work. In practice, sulphur is removed prior to steam reforming or methane synthesis to avoid catalyst poisoning, whilst a minimum concentration of hydrogen sulphide is required in the hydropyrolysis step.

2.5.3. Reforming and water-gas-shift

The reforming step aims at converting the hydrocarbon fractions into hydrogen and carbon monoxide by using high-temperature steam, in presence of a catalyst. The use of catalysts is not modelled explicitly, but the involved reactions are assumed to reach equilibrium at the reactor conditions, which are typically under 3-25 bar and 700-1100 °C. The operating parameters are set to 5 bar and 900 °C in the model, but can be varied to optimise the process performance and equipment size. An additional water-gas-shift step follows the reforming process to convert carbon monoxide. This reaction is favoured at low temperatures, in presence of catalysts. The shift process is simulated as a single stage and near-isothermal reactor at 250 °C. The use of catalysts is not modelled explicitly, but the WGS reaction is assumed to reach thermodynamic equilibrium at the reactor outlet [31,32].

2.5.4. CO_2-separation

The model of the CO_2-capture units with amines (chemical absorption) was developed using the commercial flowsheeting software Aspen Plus® version 7.2 [33], based on the electrolyte NRTL method [34] for the liquid phase and the Redlich-Kwong EOS [35] for the vapour phase. Carbon dioxide removal processes through absorption are based on local heat and mass transfers and depend as well as on the geometry of the separation columns. All absorption models are developed for steady-state conditions, accounting for the diffusion and absorption kinetics. The absorber and scrubber were modelled as rate-based instead of steady-state equilibrium, taking into account the reaction kinetics. Each column is modelled as a number of control volumes where each phase is perfectly mixed in each volume. Vapour-liquid equilibrium is assumed only at the contact interface, the heat-transfer coefficients are assumed constant, and the mass transfer is assumed to be limited by the low-flux mass-transfers. The absorption and desorption temperatures were set to 40 °C and 120 °C.

The models of the CO_2-capture units with DEPG (physical absorption) were developed using the PC-SAFT equation of state [36]. The absorber was modelled as rate-based, while the flash tanks were represented by simple phase separators with interstage flashing. The absorption temperature was set to 25 °C for an operating pressure of 22 bar to ensure high CO_2 partial pressure, while the final desorption pressure was set to 1.1 bar. Two intermediate desorption stages were considered, operating at 3 bar and 8 bar to ensure equal pressure ratios. In all cases, the solvent-to-carbon ratios were adjusted to ensure a CO_2-removal efficiency of 95 %, which corresponds to state-of-the-art CO_2-capture systems.

2.5.5. *Char valorisation*

Char combustion aims at providing the heat required in the system, which is at high ($\simeq 900\,°C$, if reforming is implemented) or moderate temperatures ($\simeq 120\,°C$, if CO_2 is removed by chemical absorption). Air is processed at near-atmospheric conditions, and the excess ratio was adjusted to ensure an exhaust temperature of 1200 °C. Air preheating is implemented to minimise the quantity of heat wasted with the exhaust gases. Higher temperatures may be achieved in practice depending on the reactor material. The reactions were assumed total, meaning that carbon is fully converted into carbon dioxides.

Char gasification consists of chemical reactions in parallel - the overall process is governed by heat- and mass-transfer phenomena in homogeneous and heterogeneous phases, and is limited by chemical kinetics. The gas composition at the gasifier outlet is generally determined by assuming chemical equilibrium at the given operating conditions. The approach selected in this work was to specify an equilibrium temperature of 725 °C and a constant carbon conversion of 90 % [37]. A methanation catalyst should be used to ensure a methane outlet content close to equilibrium.

2.5.6. *Methane synthesis*

Methanation reactions are equilibrium reactions that are favoured at low temperatures, typically about 250 °C, and at moderate pressures, usually until 30 bar. The gas composition at the reactor outlet can therefore be computed by calculating the equilibrium concentrations and adjusting the syngas composition to account for a possible deviation to equilibrium. However, as demonstrated in experimental studies, the assumption of chemical equilibrium is reasonable if the amount of catalytic material is sufficient [38]. Neglecting the formation of ethene and other by-products, the stoichiometric number (SN), i.e. the relation between the amounts of hydrogen and carbon oxides in the system, that gives the maximum methane yield obeys the following law:

$$\mathrm{SN} = \frac{\tilde{c}_{\mathrm{H2}} - \tilde{c}_{\mathrm{CO2}}}{\tilde{c}_{\mathrm{CO}} + \tilde{c}_{\mathrm{CO2}}} = 3$$

The methanation reactor is assumed to be a near-isothermal reactor at 300 °C [32,38], which results in a CO_2-conversion to CH_4 higher than 98 % at pressure levels higher than 10 bar. The hydrogen inflow is adjusted to match the optimal stoichiometric number of 3 (2.5.6) [31,32].

2.5.7. *Methanol production*

Methanol synthesis reactions are as well favoured at low temperatures, typically about 250 °C, and at high pressures, up to 100 bar in industrial applications. Chemical equilibrium is not reached and a temperature approach of 3.6 °C is considered to account for the deviation to equilibrium [32]. Copper-based catalysts are standard in industrial applications, and it is preferable to process carbon monoxide instead of carbon dioxide in this case. The synthesis reactor is assumed to be a near-isothermal reactor at 250 °C [26,32], and the hydrogen inflow is adjusted to match the optimal stoichiometric number of 2 (2.5.6). The outflow gases are condensed and cooled to 25 °C, and the recovered gases are recycled into the synthesis reactor, after a purge of 5 % and preheating to 200 °C.

2.5.8. Electrolysis

Hydrogen may be produced by low- or high-temperature electrolysis as an alternative to the reforming and water-gas-shift processes. The detailed physical and chemical phenomena are not modelled in details, and both types of electrolysers are represented by black-box models with mass and energy balances. Complete conversion of water into molecular hydrogen and oxygen is assumed, as well as constant current density and isothermal conditions. The stack pressure is taken equal to the system pressure of 22 bar. Alkaline electrolysers generally operate between 60 °C and 80 °C, for an efficiency ranging between 52 % and 69 %. High-temperature electrolysers typically operate between 700 °C and 900 °C, for an efficiency above 90 %. Operating temperatures of 80 °C and 750 °C are selected for low- and high-temperature electrolysis, for a corresponding efficiency of 64 % and 95 %, depending on the preheating temperature [19,20].

2.5.9. Energy integration

The goal of energy integration is to minimise the energy demands of a given system by maximising the internal heat recovery and optimising the operating conditions of each process. The use of external utilities, such as boilers and refrigeration cycles, should be minimised to avoid additional costs and electricity consumption. The first step is to identify the hot and cold streams, i.e. the flows that require cooling or heating, of each process, as well as their corresponding temperature levels and loads. The second step is to define an individual temperature approach for each stream ($\Delta T/2$), which defines the minimum heat transfer driving force to design a feasible and economical heat exchanger. Individual temperature approaches of 5 °C, 10 °C and 20 °C are assumed for condensing/evaporating, liquid and gaseous streams. The third step is to calculate the minimum energy requirements of the system and to optimize the size and placement of each utility.

In the present case, heat is required in (i) the production of steam for gasification, reforming, water-gas-shift and electrolysis (solid oxide); (ii) the steam reforming process; (iii) the CO_2-capture unit (if chemical absorption) and (iv) the preheating of the process gases. It is released from (i) the methanation, water-gas-shift and methanol synthesis; (ii) the electrolysis units (if alkaline); (iii) the cooling and partial condensation of the process gases. High-temperature heat can be produced by burning char or a fraction of the non-condensable gases from the PSA, or by electrical heating. Low- to moderate-temperature heat may be provided by internal heat recovery or by further exploiting the waste heat of the combustion exhausts.

2.6. Performance indicators

The performance of each layout depends on the efficiency of each process operation and on the overall system integration. The former is related to the type of product (e.g. SNG, H_2, MeOH), to the selection of a given technology (e.g. chemical or physical absorption for CO_2-removal) and of its operating conditions (e.g. temperature and pressure). The latter is related to the design of the heat recovery system and to the integration of the external heating and cooling utilities.

The system efficiency η_{system} (Equation 1) is defined as the ratio of the useful energy outputs (e.g. chemical energy of bio-oil and fuels) to the necessary energy inputs (e.g. chemical energy of biomass). The system efficiency includes the demands of hydrogen, power and heat, where the processes used to generate hydrogen and external heating are not accounted for.

$$\eta_{\text{system}} = \frac{\Delta h^0_{\text{bio-oil}} \cdot \dot{m}_{\text{bio-oil}} + \Delta h^0_{\text{SNG}} \cdot \dot{m}_{\text{SNG}} + \Delta h^0_{\text{H}_2,\text{produced}} \cdot \dot{m}_{\text{H}_2,\text{produced}} + \Delta h^0_{\text{MeOH}} \cdot \dot{m}_{\text{MeOH}}}{\Delta h^0_{\text{biomass}} \cdot \dot{m}_{\text{biomass}} + \Delta h^0_{\text{H}_2,\text{external}} \cdot \dot{m}_{\text{H}_2,\text{external}} + \dot{W}_{\text{external}} + \dot{Q}_{\text{external}}} \tag{1}$$

where $\dot{m}$, Δh^0, $\dot{W}$ and $\dot{Q}$ are the mass flow rates, lower heating values, power and heat demands.

A total efficiency (Equation 2) is defined: it considers the electrical losses in the upstream processes to generate the hydrogen and heat required on-site.

$$\eta_{\text{total}} = \frac{\Delta h^0_{\text{bio-oil}} \cdot \dot{m}_{\text{bio-oil}} + \Delta h^0_{\text{SNG}} \cdot \dot{m}_{\text{SNG}} + \Delta h^0_{\text{H}_2,\text{produced}} \cdot \dot{m}_{\text{H}_2,\text{produced}} + \Delta h^0_{\text{MeOH}} \cdot \dot{m}_{\text{MeOH}}}{\Delta h^0_{\text{biomass}} \cdot \dot{m}_{\text{biomass}} + \dot{W}_{\text{total}}} \tag{2}$$

If the produced char is not converted, both efficiencies will also be given with a term $\Delta h^0_{\text{char}} \cdot \dot{m}_{\text{char}}$.

Finally, a carbon conversion efficiency (Equation 3) is derived (X_{C}), defined as the ratio of carbon present in the valuable outputs (e.g. bio-oil, SNG and CH_3OH) to the carbon introduced in the system with biomass:

$$X_{\text{C}} = \frac{x_{\text{C,bio-oil}} \cdot \dot{m}_{\text{bio-oil}} + x_{\text{C,SNG}} \cdot \dot{m}_{\text{SNG}} + x_{\text{C,MeOH}} \cdot \dot{m}_{\text{MeOH}}}{x_{\text{C,biomass}} \cdot \dot{m}_{\text{biomass}}} \tag{3}$$

3. Results

The results from the modelling of the polygeneration systems based on catalytic hydropyrolysis are presented and commented in the following section. Sizing of the polygeneration systems is not within the scope of this paper, and all systems are therefore based on a 100 MWth biomass input (LHV).

3.1. Standard system

The standard hydropyrolysis system for production of bio-oil through hydropyrolysis is presented in Figure 3 with the corresponding data in Table 3.

Table 3: Process data of the polygeneration system for production of bio-oil through hydropyrolysis and hydrodeoxygenation with internal generation of hydrogen and a burner.

Node	m (kg/s)	T (°C)	p (bar)	Node	m (kg/s)	T (°C)	p (bar)
1	5.76	25	22.4	18	1.15	219	5
2	3.46	25	22.4	19	1.30	152	5
3	9.22	25	22.4	20	0.95	152	5
4	0.52	429	22.4	21	2.45	170	5
5	8.70	429	22.4	22	2.45	750	5
6	8.70	363	22.4	23	2.45	900	5
7	8.70	367	22.4	24	2.45	250	5
8	8.70	25	22.4	25	3.40	224	5
9 {bio-oil}	1.57	25	22.4	26	3.40	200	5
9 {water}	2.24	25	22.4	27	3.40	40	5
10	4.91	25	22.4	28	2.03	40	5
11	2.87	25	22.4	29	0.42	40	5
12	2.04	25	22.4	30	0.42	223	22.4
13	0.17	25	22.4	31	0.42	25	22.4
14	1.87	25	1.1	32	10.7	25	1.1
15	0.72	25	1.1	33	10.7	950	1.1
16	1.15	25	1.1	34	11.4	1000	1.1
17	1.15	125	5	35	0.94	40	5

The analysis of the chemical energy flows of the hydropyrolysis system (Figure 4) illustrates the chemical transformations from biomass to bio-oil and shows that this system can be self-sufficient in terms of hydrogen and heat. The light gases have an energy content of about 40 % of the biomass input (LHV), which is slightly higher than the combined demand of hydrogen (29.5 %) and heat (6 %). This figure also shows that the core hydropyrolysis process is very energy-efficient, only having a chemical energy loss equivalent to 8.4 % of the biomass input. The waste heat contained in the burner exhausts amounts to 12 % of the feed energy content and could be valorized in Rankine cycles or used in other heating systems, since the exhausts have a temperature above 900 °C. The power demand is negligible, as all process units, except for the burner, operate at 22.4 bar, and the system efficiency is about 61 % if char is not included, and 76 % otherwise. In practice, some electricity would be required for pressurising the biomass and compressing the recirculated gases because of the pressure drops. The carbon efficiency is about 49 % if char is not included, and 63 % otherwise.

The temperature-enthalpy curves (grand composite) of the hydropyrolysis system (Figure 5) show that the heating demand corresponds to the reforming process, which is satisfied by burning a fraction of the non-condensable gases. The cooling demand takes place near ambient conditions, and is met by processing cooling water. The steam production for the reforming process can be satisfied internally: heat is recovered from the water-gas-shift process, available at 250 °C, to preheat and evaporate the water, and from the cooling of the gases at the outlet of the pyrolysis and reforming steps, for further superheating.

3.2. SNG production

Different alternatives for char valorisation ('SNG-C' and 'SNG-G', for combustion and gasification), reformer heating, CO_2-separation ('SNG-PA' and 'SNG-CA', for physical and chemical absorption) and H_2 production ('SNG-R' and 'SNG-E', for reforming and electrolysis) were considered for the system layouts with SNG by-production, and their performances are reported in Table 4.

The selection of the CO_2-capture process has a considerable impact on the opportunities for energy integration and system efficiency. The integration of a chemical absorption process increases the heating demand of the entire system (7 to 11 MW per 100 $MW_{biomass}$), and this energy need cannot be fully satisfied with heat recovery from the cooling of the process gases and methanation processes. It can either be met by burning char (Figure 6), which results in a smaller SNG production ('SNG-R-C-CA'), or by additional electrical heating ('SNG-R-G-CA'). The latter is presented in details in Appendix B.

The integration of a physical absorption unit ('SNG-R-G-PA') eliminates the need for heating at low and moderate temperature levels - external heating is then only required to drive the reforming process. The latter is presented in details in Appendix C. The system efficiency increases by up to 4 %-points, as the power demand of the Selexol CO_2-capture process is smaller than the heating demand of the MEA one. A comparison of the temperature-enthalpy curves of these two systems (Figure 7) illustrates the possibilities for energy integration. In theory, as the pinch point is located at the amine regeneration temperature, excess heat from below the pinch can be lifted above through a heat pump. This would result in a better energy integration of the MEA CO_2-capture unit, but reveals infeasible in practice as high temperature lifts are required.

The configurations 'SNG-R' are characterised by the internal production of hydrogen. Alternatively, hydrogen can be produced through electrolysis, giving the possibility to integrate electricity from renewable energies. Such systems ('SNG-E') present very different power and heat demands. The external heating demand is negligible, but the power demand increases significantly with the electrolysis process. The use of alkaline electrolysers ('SNG-E-G-AE') results in a large discharge of waste heat at 80-90 °C, which should either be removed by using cooling water or low-temperature district heating. The implementation of solid oxide units ('SNG-E-G-SE') is beneficial as these components display a higher efficiency than alkaline electrolysers, and they can benefit from a close integration with the other processes. The steam required in

Table 4: Performance of polygeneration systems with SNG production

Layout	SNG-R	SNG-R-C -CA	SNG-R-G -CA	SNG-R-G -PA	SNG-E -SE	SNG-E-G -SE	SNG-E-G -AE
Pathway							
Product	SNG	SNG	SNG	SNG	SNG	SNG	SNG
H_2	R	R	R	R	E	E	E
Char	-	C	G	G	-	G	G
Technologies							
CO_2	CA	CA	CA	PA	-	-	-
Electrolysis	-	-	-	-	SE	SE	AE
Inputs (MW)							
Biomass	100	100	100	100	100	100	100
Heat (reformer)	9	-	11	11	-	-	-
Heat (others)	4	-	6	-	-	-	-
Hydrogen	-	-	-	-	49	63	63
Electricity	2(15)	2(2)	3(20)	3(15)	0(51)	0(66)	0(117)
Outputs (MW)							
Bio-oil	61	61	61	61	61	61	61
SNG	18	18	31	31	59	83	83
Char	15	-	-	-	15	-	-
Efficiency							
η_{system}	68 %	77 %	77 %	81 %	79 %	89 %	89 %
$\eta_{\text{system,char}}$	81 %	-	-	-	91 %	-	-
η_{total}	68 %	77 %	77 %	81 %	79 %	88 %	67 %
$\eta_{\text{total,char}}$	81 %	-	-	-	89 %	-	-
X_{C}	59 %	59 %	70 %	70 %	86 %	98 %	98 %
$X_{\text{C},char}$	73 %	-	-	-	100 %	-	-

the SOEC can be generated by recovering heat from the methanation process and the cooling of gases from the hydrodeoxygenation, which reduces the need for external cooling. It can further be superheated close to the electrolysis temperature by using the heat of the hydrogen and oxygen streams yielded by the SOEC. The flow diagram and data of the layout 'SNG-E-G-SE' are presented in details in Appendix D.

The highest carbon conversion efficiencies are reached when electrolysis is implemented (86-100 % compared to 59-73 %), as the only possible sources of carbon losses in this case are the ash/char streams. Hydrogen generation through reforming of the non-condensable light gases results in losses of up to 27 % of the biomass carbon with the carbon dioxide recovered in the absorption unit.

3.3. H_2 production

Molecular hydrogen can be generated as a final product instead of SNG, although the number of possible configurations is more limited, as the use of electrolysis is not relevant. Moreover, producing hydrogen without adding a char gasification unit has limited benefits, since most light gases are reformed to sustain the hydrogen demand of the hydropyrolysis section. Two configurations are assessed, with either chemical ('H2-R-G-CA') or physical ('H2-R-G-PA') absorption for separating carbon dioxide. The flow diagram and data of the layout 'H2-R-G-CA' are presented in details in Appendix E.

The major heating demands correspond to the reforming and amine regeneration processes, which is expected as the layout of H_2-production systems is strongly similar to SNG-production ones. Both increase in comparison to the SNG cases, since all carbon oxides are processed through the reforming section instead of being converted into methane. The Selexol process is even more attractive, since the difference in system efficiency increases from 4 to 9 %-points when substituting the MEA unit. The carbon conversion efficiency of H_2-generation processes is the lowest of all polygeneration systems investigated in this work.

3.4. MeOH production

Methanol can be produced by converting the carbon monoxide present in the reformed gas after compression and synthesis at high pressure, and its yield can be maximised by capturing and recycling the carbon dioxide to the reformer. As for SNG and H_2 production systems, either physical ('MeOH-PA') or chemical absorption ('MeOH-CA') can be integrated to remove carbon dioxide. In both cases, the syngas from the reformer are split into two processing routes: a first one where the hydrogen required in the hydropyrolysis is generated through water-gas-shift and CO_2-capture, and a second one where the remaining syngas is compressed and converted into methanol. The flow diagram and data of the layout 'MeOH-R-G-CA' are presented in details in Appendix F.

The advantage of implementing an electrolysis unit is studied considering solid oxide electrolysers ('MeOH-E-SE'). No water-gas-shift reactor is required, but a reforming unit is still needed to achieve the desired stoichiometry between hydrogen and carbon monoxide. The integration of the Selexol process results in an increase of the system performance by about 4 %-points, and the implementation of electrolysis gives a further increase of 4 %-points. The heat required to generate the steam used in the reforming process can be recovered from the methanol synthesis unit, while the heat demand of the amine reboiler can be

Table 5: Performance of polygeneration systems with H_2 and MeOH production

Layout	H2-R-G-CA	H2-R-G-PA	MeOH-R-G-CA	MeOH-R-G-PA	MeOH-E-G-PA-SE
Pathway					
Product	H_2	H_2	MeOH	MeOH	MeOH
H_2	R	R	R	R	E
Char	G	G	G	G	G
Technologies					
CO_2	CA	PA	CA	PA	PA
Electrolysis	-	-	-	-	SE
Inputs (MW)					
Biomass	100	100	100	100	100
Heat (reformer)	18	18	19	19	19
Heat (others)	16	-	8	-	-
Hydrogen	-	-	-	-	42
Electricity	5(39)	5(23)	6(33)	8(27)	7(70)
Outputs (MW)					
Bio-oil	61	61	61	61	61
Hydrogen	37	37	-	-	-
Methanol	-	-	33	33	68
Efficiency					
η_{system}	71 %	81 %	71 %	74 %	78 %
η_{total}	71 %	81 %	71 %	74 %	76 %
X_{C}	49 %	49 %	71 %	71 %	95 %

fully satisfied only by implementing electrical heating. The flow diagram and data of the layout 'MeOH-E-G-SE' are presented in details in Appendix G. Similar carbon conversion efficiencies are reached with MeOH production as with SNG generation. A value of 95 % is reached when combining electrolysis and char gasification. This is a few percentage points lower than for SNG, since carbon is lost with the purge after the MeOH-synthesis reactor.

4. Discussion

The standard system, which is characterised by the production of bio-oil and recirculation of the light gases, displays an efficiency η_{system} of 61 % and is self-sufficient in terms of heat and power. The steam reformer can be heated by burning either char or a fraction of the reformed gases, and the two options are equivalent efficiency-wise.

The results show a higher energy efficiency of polygeneration systems that produce SNG, H_2 and MeOH compared to the standard system, in all cases, whether hydrogen is produced internally or externally, and whether electrical heating or char combustion is required to satisfy the demand of the reforming process. The increase in system efficiency is of 7 to 28 %-points when producing SNG, 10 to 21 %-points when producing H_2, and 10 to 17 %-points when producing MeOH. The smallest improvement (7 %-points) is observed when all the light gases are recirculated and reformed, while a fraction of char is burnt to heat the reformer. The highest improvement (28 %-points) is reached when electrolysis is used to cover the hydrogen demand and char is valorized through gasification and SNG production. The systems co-producing SNG reach the highest system efficiency because methane, ethane and propane are generated inside the core hydropyrolysis process. Very limited upgrading is therefore needed to convert all the light gases to SNG.

The configurations with H_2-production by char gasification can reach a system efficiency up to 80 %, which is sensibly similar (81 %) to layouts with SNG production, using reforming, and with the same heating and CO_2-capture systems. Systems with MeOH production cannot reach as high efficiencies - they are penalized by the added processing. The power consumption increases significantly because of the compression process to 96 bar, while the heating demand increases with the inclusion of a reformer and CO_2-capture unit with greater processing capacities. Despite the lower efficiency, co-production of methanol could be attractive from an economical point of view, as methanol is generally valued higher than SNG or hydrogen.

The total efficiency η_{total}, including the losses occurring in the electrolysis and electricity heating systems, is lower than the system efficiency by 0 to 2 %-points, except when hydrogen is generated by alkaline electrolysis. The biggest drop occurs when hydrogen is produced in alkaline electrolysers. In this case, the total efficiency is 22 %-point lower than the system efficiency (comparison of SNG-E-G-SE and SNG-E-G-AE systems). No difference between the system and total efficiencies is observed when hydrogen is generated internally and char is burnt to heat the reformer.

The selection of the CO_2-capture unit has a considerable impact on the system design and performance. In all cases, the CO_2-removal process by chemical absorption with MEA is a large heat sink. The heat requirements cannot be satisfied by heat recovery from other process units, and electrical heating should be implemented, which results in lower efficiencies. The highest penalty is found for the system configurations producing MeOH. The grand composite curves (see e.g. Figure 7) demonstrate graphically these limitations, as the pinch point is located at the amine regeneration temperature. Firstly, there is no excess heat at high temperatures that can be valorized through, for example, Rankine cycles. Secondly, in theory, excess heat from below the pinch could be transferred to higher temperatures through heat pumps, which would decrease the heat demand of the MEA process. However, such solutions are impracticable: little heat is available in the range 105-120 °C, and large temperature lifts are not feasible.

The integration of alternative CO_2-removal methods, such a physical absorption, eliminates the heat demand at low temperatures in all scenarios. The system efficiency is higher by 4 to 10 %-points if MEA absorption processes are replaced, and the polygeneration systems become self-sufficient, excluding the steam reforming needs. The grand composite curves show that the pinch point is located at the reforming temperature for such configurations. The system efficiency could be improved by implementing a Rankine cycle (steam or organic) to convert the high- and moderate-temperature heat into power, which may be promising in large-scale applications, or by producing district heating water. Finally, using solid oxide electrolysers is more beneficial than implementing alkaline electrolysers. SOECs present higher electricity-to-hydrogen efficiencies and benefit from synergies with the other processes present in the polygeneration system (steam can be generated internally).

5. Conclusion

In this paper, novel polygeneration concepts based on catalytic hydropyrolysis and hydrodeoxygenation were analysed and compared via process simulation and thermodynamic analysis. These systems have the potential of converting biomass into high-quality bio-oil, liquid (MeOH) and gaseous (SNG and H_2) fuels - and flowsheet models of twelve promising layouts were developed based on literature and industrial data. The possibilities for improving their performance by process and energy integration were investigated in details. A standard hydropyrolysis system without additional fuel co-generation displays an efficiency in the range of approximately 61 % (LHV), based on a representative published experiment (GTI). The system performance is increased by 7 to 28 %-points when co-producing SNG, 10 to 21 %-points when producing H_2, and 10 to 17 %-points when producing MeOH. Carbon conversion efficiencies are highest when generating SNG or MeOH and reach a maximum when electrolysis is implemented (98 % and 95 %), since there are no carbon losses associated with the CO_2-separation process. SNG production systems present higher energy efficiency compared to H_2 and MeOH ones, as they require less processing. Besides the choice of the by-product, the plant performance is strongly dependent on the selection of the CO_2-separation process and electrolysis unit. Systems with chemical absorption suffer from a large heating demand at low temperature level, which can be satisfied only by burning bio-char, or, in most cases, by electrical heating. Systems with solid oxide electrolyser cells benefit from synergies with the fuel synthesis processes, using waste heat for steam production. The presented results highlight the potential of polygeneration, in this case for hydropyrolysis based systems, and furthermore shows the potential for input of renewable electricity in fuels and chemicals production. However, the increases in efficiency come at the expense of more complex plant designs, and detailed economic analyses are needed to evaluate the competitiveness of each option.

Acknowledgements

The funding from the Innovation Fund Denmark - Innovationsfonden, within the H2CAP (Hydrogen assisted catalytic biomass pyrolysis for green fuels) project, is acknowledged.

Appendix A. Experiment 5/25

The so-called experiment 5/25 used maple fed for 18.4 hours [29]. The weight recovery, relative to biomass, on a dry and ash-free basis, was 103.9 % with a carbon recovery of 98.6 %. The yields were 27.9 % for liquid hydrocarbons (C_4^+), 15.6 % for light hydrocarbons (C_1-C_3), 10.3 % for CO_2, 6 % for CO, 8.7 % for char and 36.1 % for water. The composition of the hydrocarbon gas is, on a weight basis, 31.3 % CH_4, 42 % C_2H_6 and 26.8 % C_3H_8. The composition of bio-oil is, on a weight basis, 87.4 % carbon, 10.9 % hydrogen, less than 1 % oxygen, and less than 0.01 % nitrogen and sulfur. The composition of char is, on a weight basis, 78.5 % carbon, 3.5 % hydrogen, 0.4 % nitrogen, and 11.7 % ash. The recovered water has about 0.6 %-wt carbon, and has a negligible content of sulfur and ammonia.

Appendix B. Polygeneration of bio-oil and synthetic natural gas, with chemical absorption (SNG-R-G-CA)

The layout of the polygeneration system SNG-R-G-CA is presented in Figure B.10 with the corresponding data in Table B.6.

Table B.6: Process data of the investigated polygeneration system for production of bio-oil and synthetic natural gas, with chemical absorption.

Node	m (kg/s)	T (°C)	p (bar)	Node	m (kg/s)	T (°C)	p (bar)
1	5.76	25	22.4	24	5.03	25	5
2	3.19	25	22.4	25	3	25	5
3	8.95	429	22.4	26	0.64	25	5
4	0.52	429	22.4	27	0.64	234	22.4
5	8.43	429	22.4	28	2.53	25	22.4
6	8.43	363	22.4	29	0.15	25	22.4
7	8.43	367	22.4	30	0.13	25	22.4
8	8.43	429	22.4	31	0.13	675	22.4
9 {bio-oil}	1.57	25	22.4	32	0.24	675	22.4
9 {water}	2.22	25	22.4	33	0.79	725	22.4
10	4.64	25	22.4	34	0.1	725	22.4
11	2.11	25	22.4	35	0.79	374	22.4
12	1.82	25	22.4	36	0.79	25	22.4
13	1.67	25	1.1	37	0.7	25	22.4
14	1.67	167	5	38	0.09	25	22.4
15	1.67	219	5	39	0.99	25	22.4
16	2	152	5	40	0.99	250	22.4
17	3.67	172	5	41	0.99	300	22.4
18	3.67	750	5	42	0.99	40	22.4
19	3.67	900	5	43	0.64	40	22.4
20	3.67	250	5	44	0.34	40	22.4
21	1.36	152	5	45	0.64	25	22.4
22	5.03	223	5	46	0.51	25	22.4
23	5.03	250	5	47	1.39	25	5

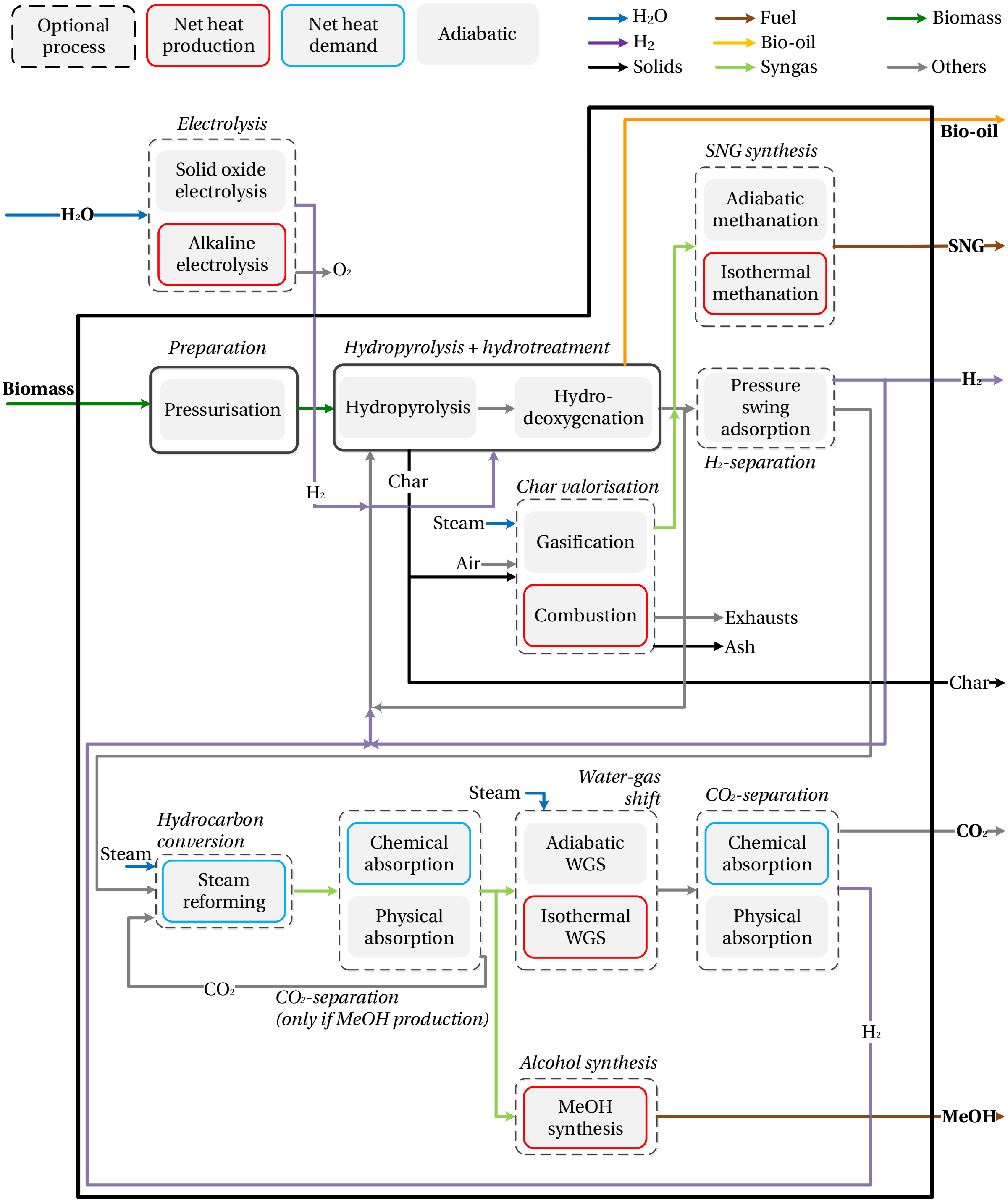

Figure 2: Superstructure of the polygeneration system for production of bio-oil, SNG, H_2 and MeOH through hydropyrolysis and hydrodeoxygenation.

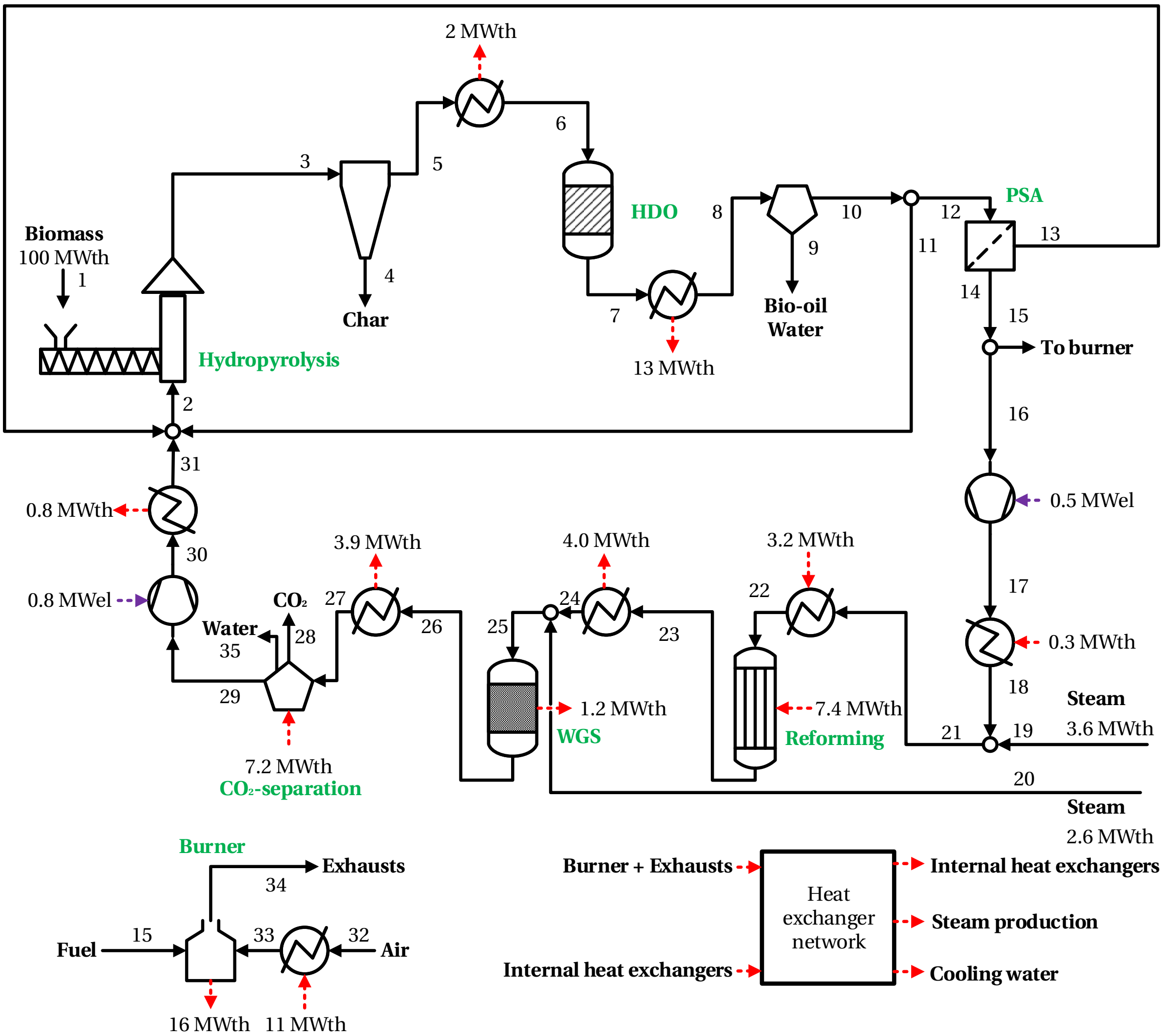

Figure 3: Flowsheet of the polygeneration system for production of bio-oil through hydropyrolysis and hydrodeoxygenation with internal generation of hydrogen and a burner.

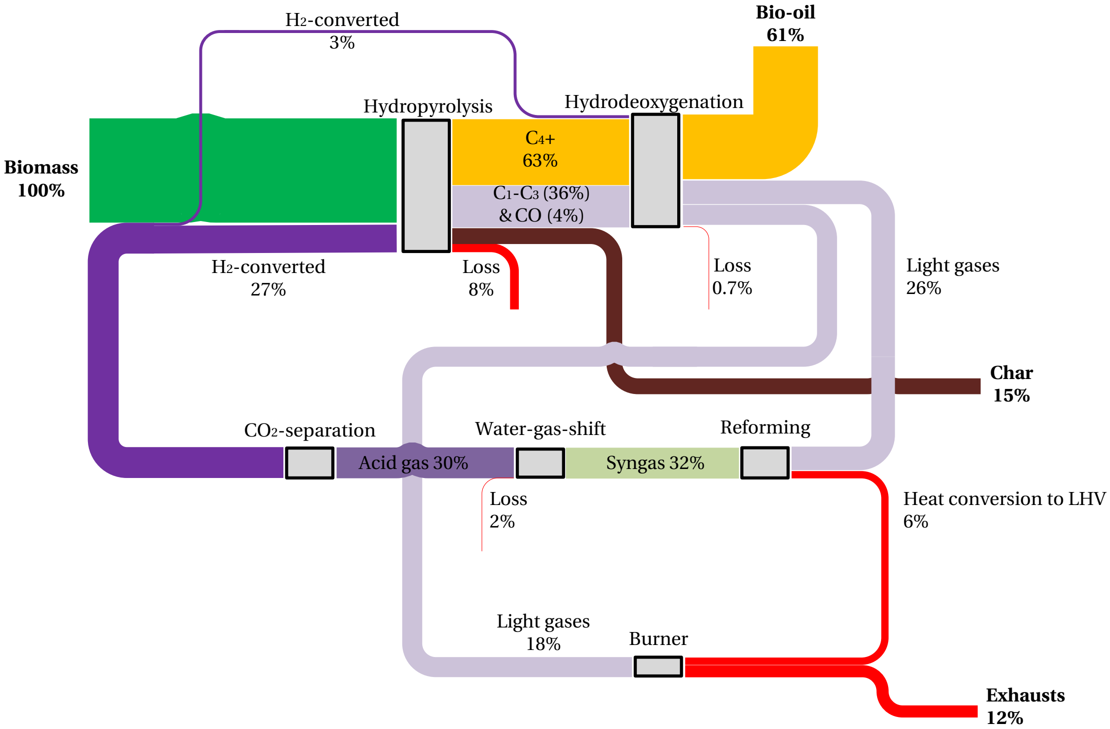

Figure 4: Sankey diagram (chemical energy flows) of the standard hydropyrolysis system.

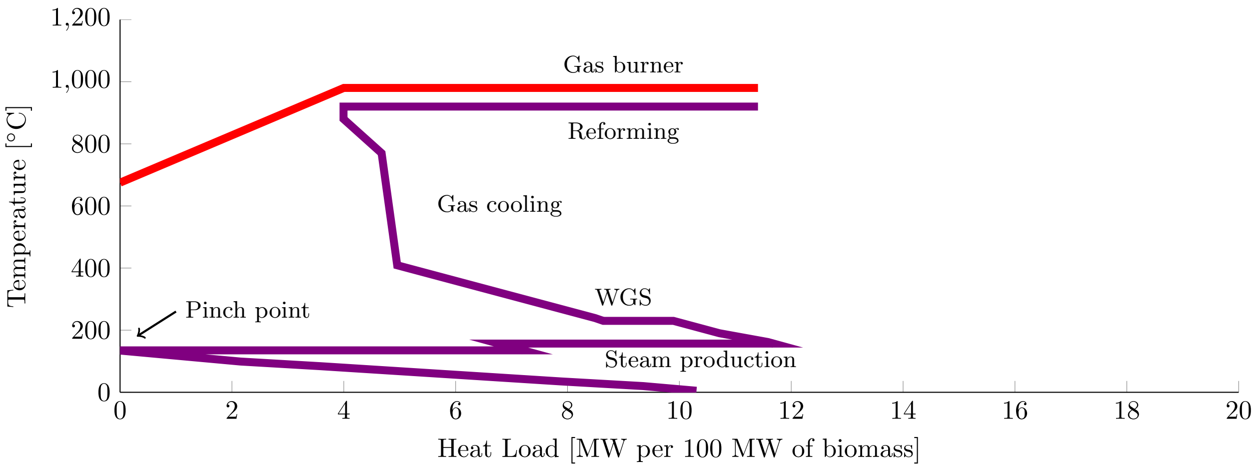

Figure 5: Composite curves for the standard hydropyrolysis system

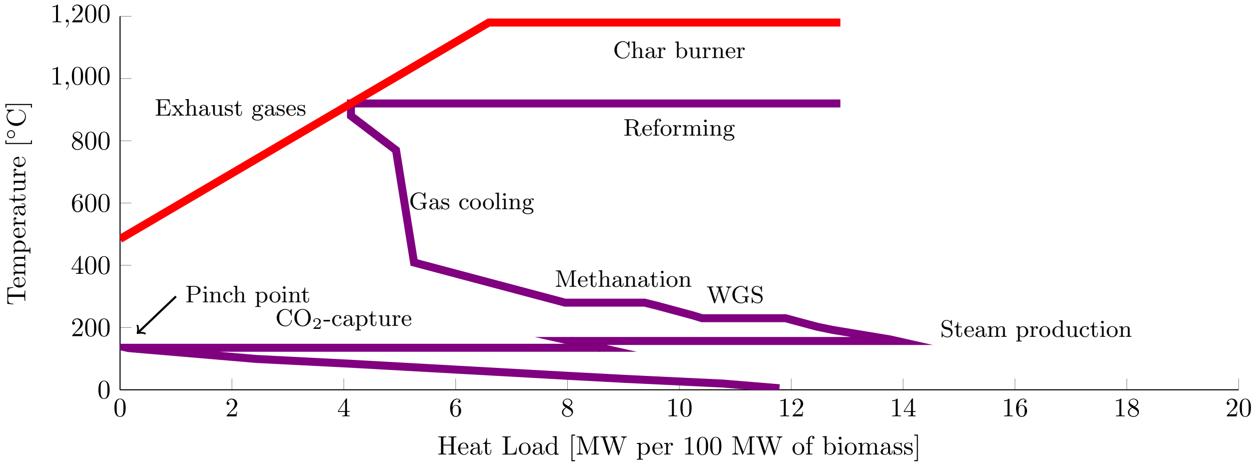

Figure 6: Composite curves for the polygeneration system with SNG production, char combustion and chemical absorption (SNG-R-C-CA)

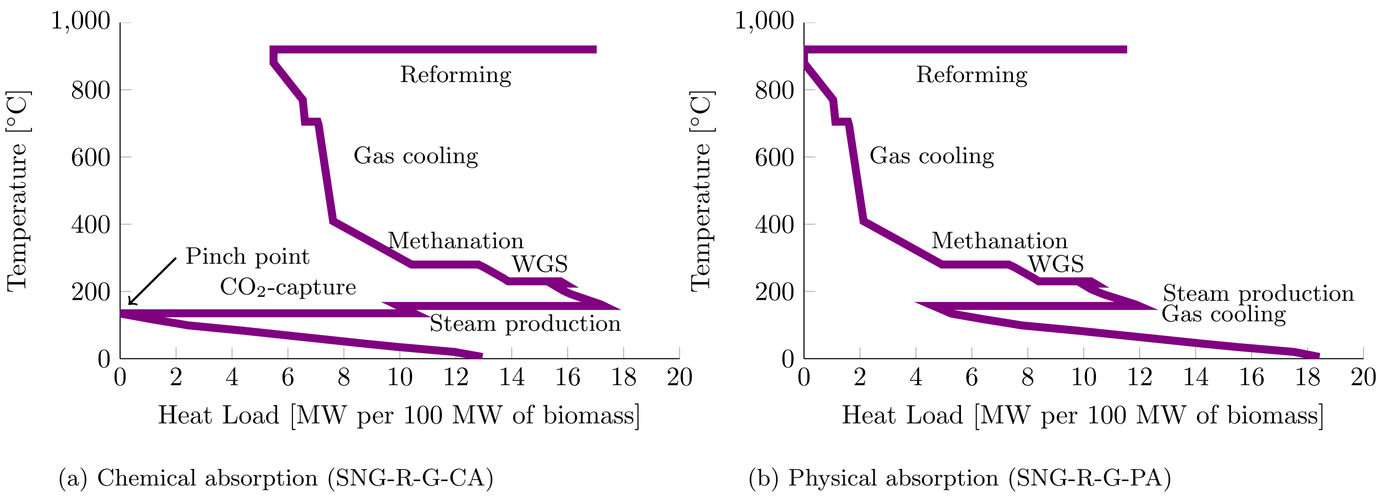

Figure 7: Composite curves for the polygeneration systems with SNG production, gas reforming and char gasification

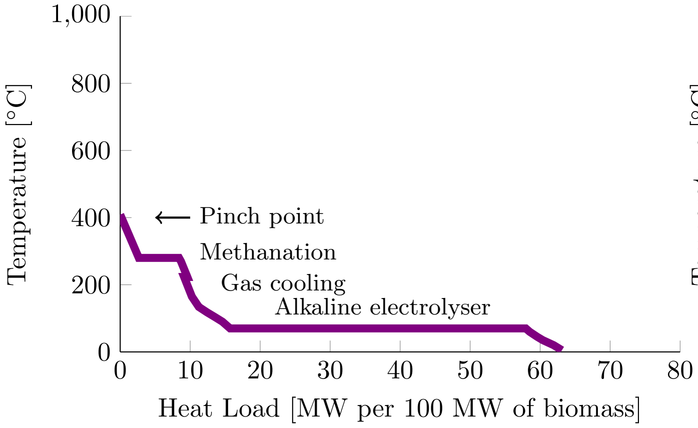

(a) Alkaline electrolysis (SNG-E-G-AE)

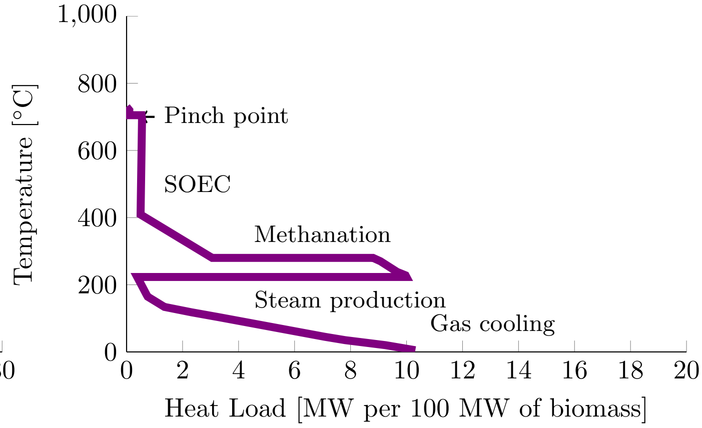

(b) Solid oxide electrolysis cell (SNG-E-G-SE)

Figure 8: Composite curves for the polygeneration systems with SNG production and electrolysis

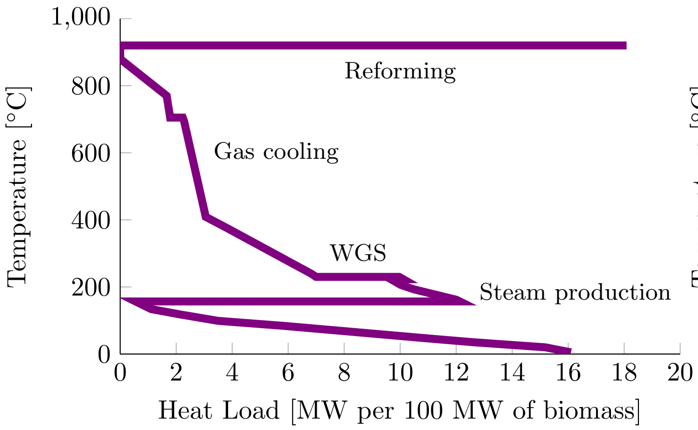

(a) H_2-production (H2-R-G-PA)

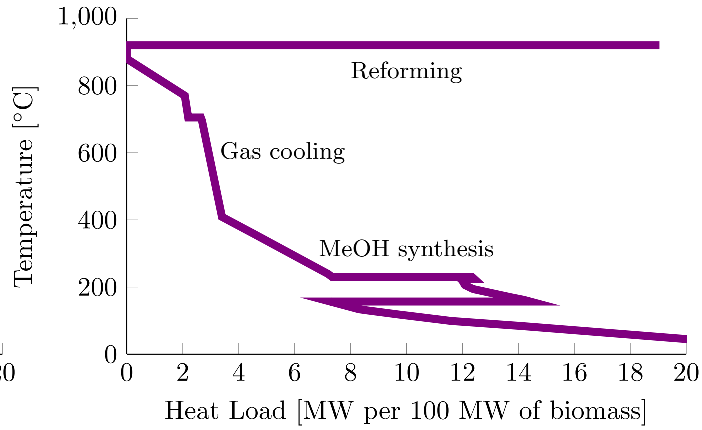

(b) MeOH production (MeOH-R-G-PA)

Figure 9: Composite curves for the polygeneration systems with H_2 and MeOH production

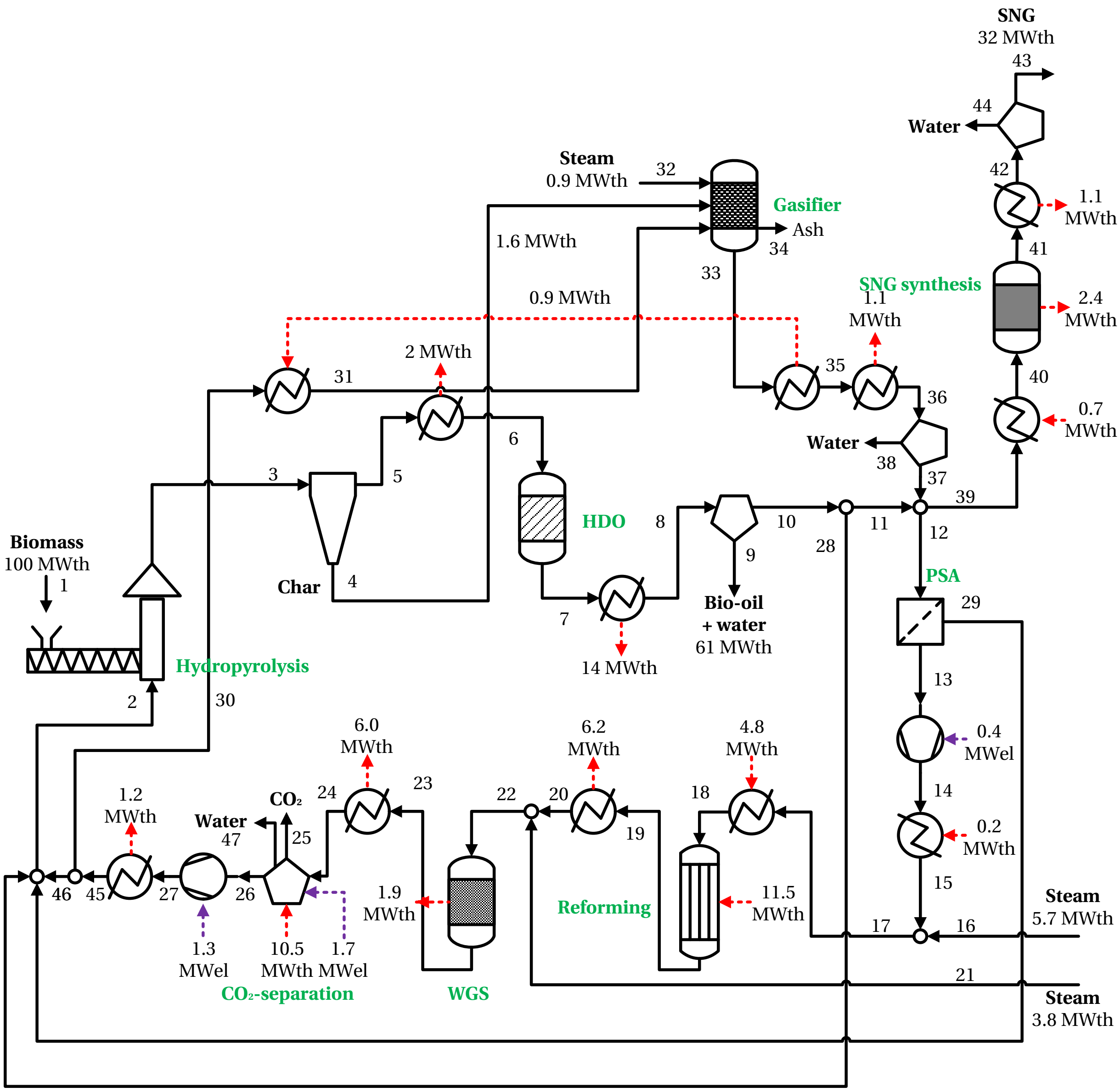

Figure B.10: Process flow diagram of the investigated polygeneration system for production of bio-oil and synthetic natural gas, with chemical absorption.

Appendix C. Polygeneration of bio-oil and synthetic natural gas, with physical absorption (SNG-R-G-PA)

The layout of the polygeneration system SNG-R-G-PA is presented in Figure C.11 with the corresponding data in Table C.7.

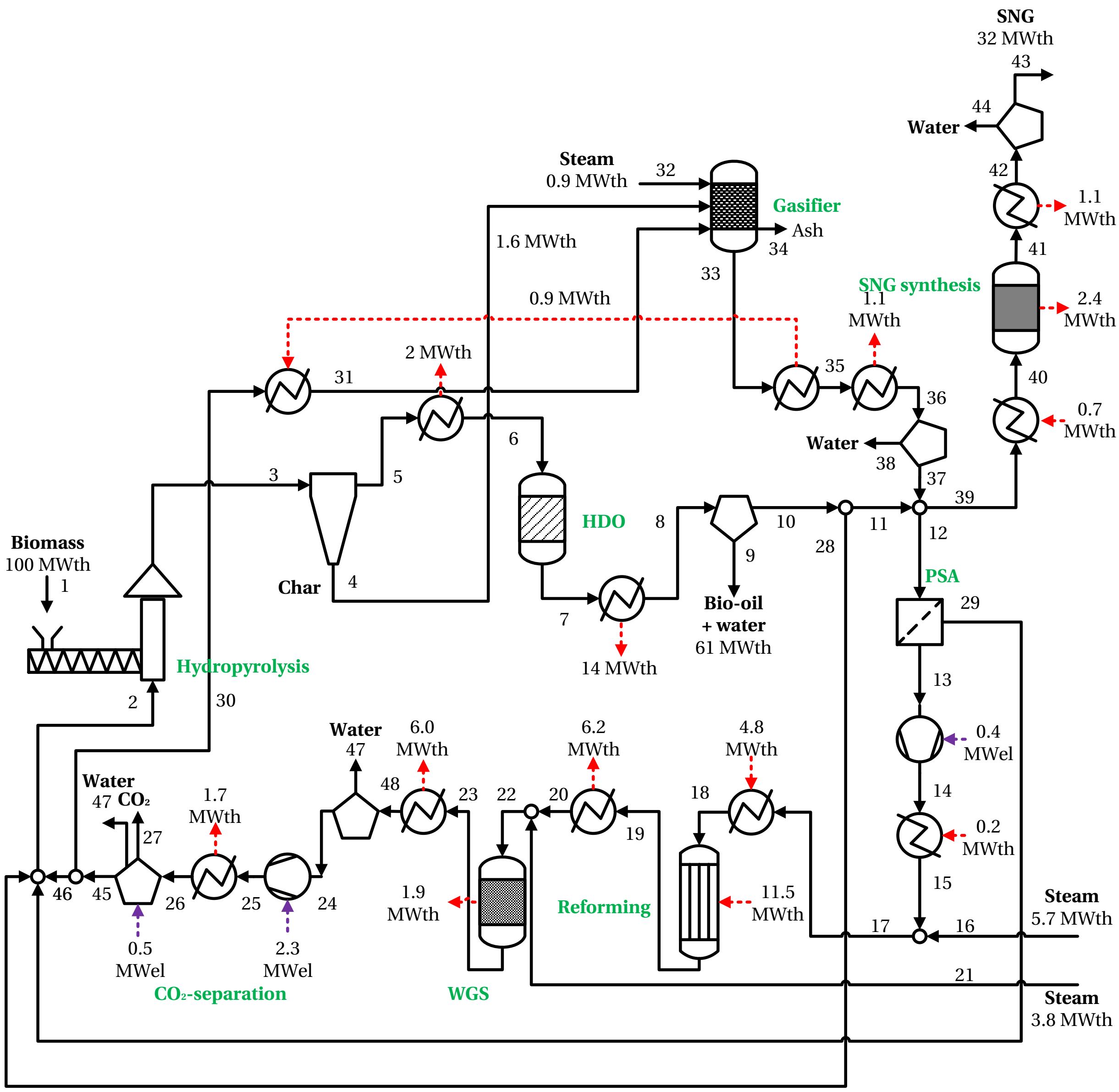

Figure C.11: Process flow diagram of the investigated polygeneration system for production of bio-oil and synthetic natural gas, with physical absorption.

Table C.7: Process data of the investigated polygeneration system for production of bio-oil and synthetic natural gas, with physical absorption.

Node	m (kg/s)	T (°C)	p (bar)	Node	m (kg/s)	T (°C)	p (bar)
1	5.76	25	22.4	24	3.64	25	5
2	3.19	25	22.4	25	3.64	215	22.4
3 0.64 3	8.95	429	22.4	26	3.64	25	22.4
4	0.52	429	22.4	27	3	25	1.1
5	8.43	429	22.4	28	2.53	25	22.4
6	8.43	363	22.4	29	0.15	25	22.4
7	8.43	367	22.4	30	0.13	25	22.4
8	8.43	429	22.4	31	0.13	675	22.4
9 {bio-oil}	1.57	25	22.4	32	0.24	675	22.4
9 {water}	2.22	25	22.4	33	0.79	725	22.4
10	4.64	25	22.4	34	0.1	725	22.4
11	2.11	25	22.4	35	0.79	374	22.4
12	1.82	25	22.4	36	0.79	25	22.4
13	1.67	25	1.1	37	0.7	25	22.4
14	1.67	167	5	38	0.09	25	22.4
15	1.67	219	5	39	0.99	25	22.4
16	2	152	5	40	0.99	250	22.4
17	3.67	172	5	41	0.99	300	22.4
18	3.67	750	5	42	0.99	40	22.4
19	3.67	900	5	43	0.64	40	22.4
20	3.67	250	5	44	0.34	40	22.4
21	1.36	152	5	45	0.64	25	22.4
22	5.03	223	5	46	0.51	25	22.4
23	5.03	250	5	47	1.39	25	5
				48	3.64	25	5

Appendix D. Polygeneration of bio-oil and synthetic natural gas, with solid oxide electrolysis (SNG-E-G-SE)

The layout of the polygeneration system SNG-E-G-SE is presented in Figure D.12 with the corresponding data in Table D.8.

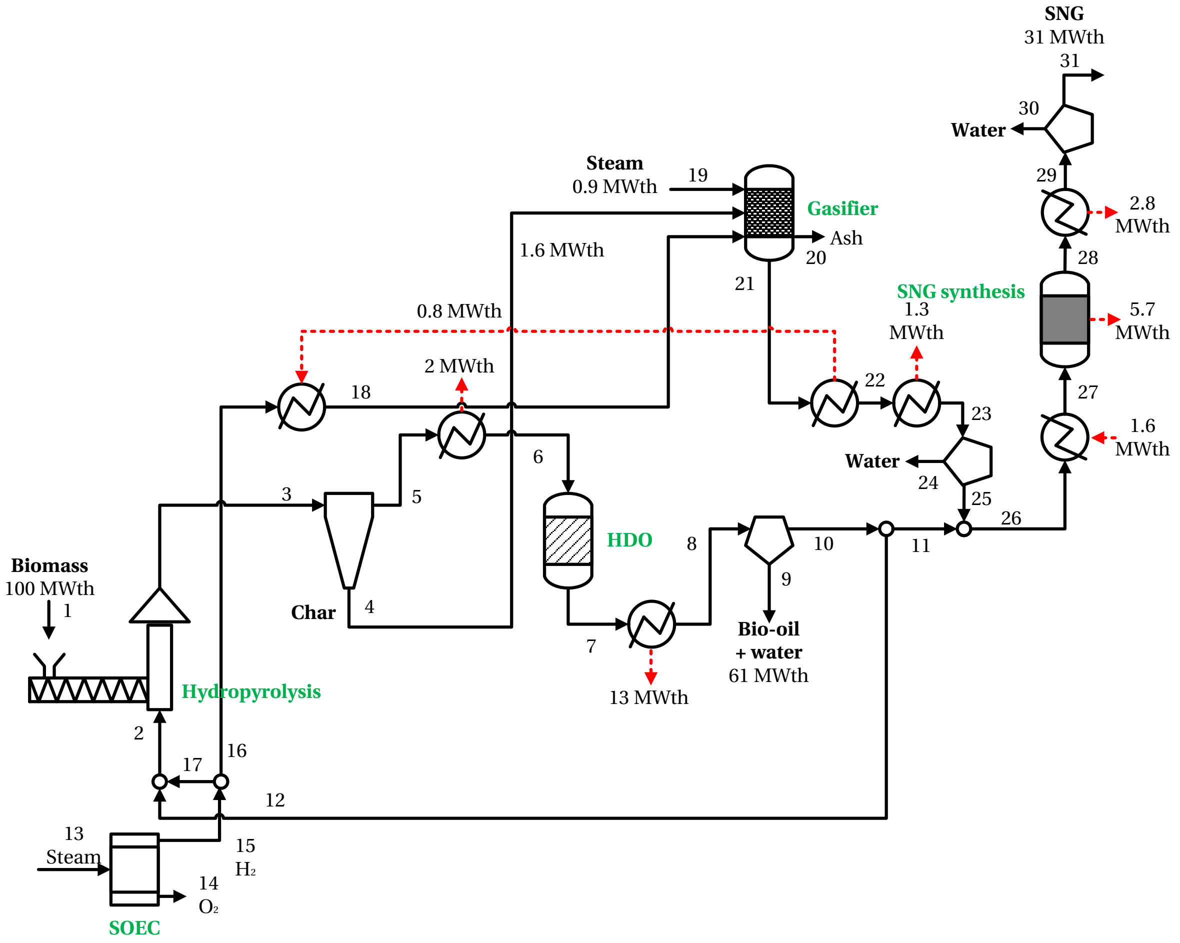

Figure D.12: Process flow diagram of the investigated polygeneration system for production of bio-oil and synthetic natural gas, with electrolysis.

Table D.8: Process data of the investigated polygeneration system for production of bio-oil and synthetic natural gas, with electrolysis.

Node	m (kg/s)	T (°C)	p (bar)	Node	m (kg/s)	T (°C)	p (bar)
1	5.76	25	22.4	16	0.09	25	22.4
2	3.26	25	22.4	17	0.44	25	22.4
3	9.02	429	22.4	18	0.09	675	22.4
4	0.52	429	22.4	19	0.24	675	22.4
5	8.5	429	22.4	20	0.1	725	22.4
6	8.5	363	22.4	21	0.75	725	22.4
7	8.5	367	22.4	22	0.75	384	22.4
8	8.5	25	22.4	23	0.75	25	22.4
9 {bio-oil}	1.57	25	22.4	24	0.09	25	22.4
9 {water}	2.22	25	22.4	25	0.65	25	22.4
10	4.71	25	22.4	26	2.54	25	22.4
11	1.88	25	22.4	27	2.54	250	22.4
12	2.82	25	22.4	28	2.54	300	22.4
13	4.69	25	22.4	29	2.54	40	22.4
14	4.17	25	22.4	30	0.81	40	22.4
15	0.52	25	22.4	31	1.72	40	22.4

Appendix E. Polygeneration of bio-oil and hydrogen, with chemical absorption (H2-G-CA)

The layout of the polygeneration system H2-G-CA is presented in Figure E.13 with the corresponding data in Table E.9.

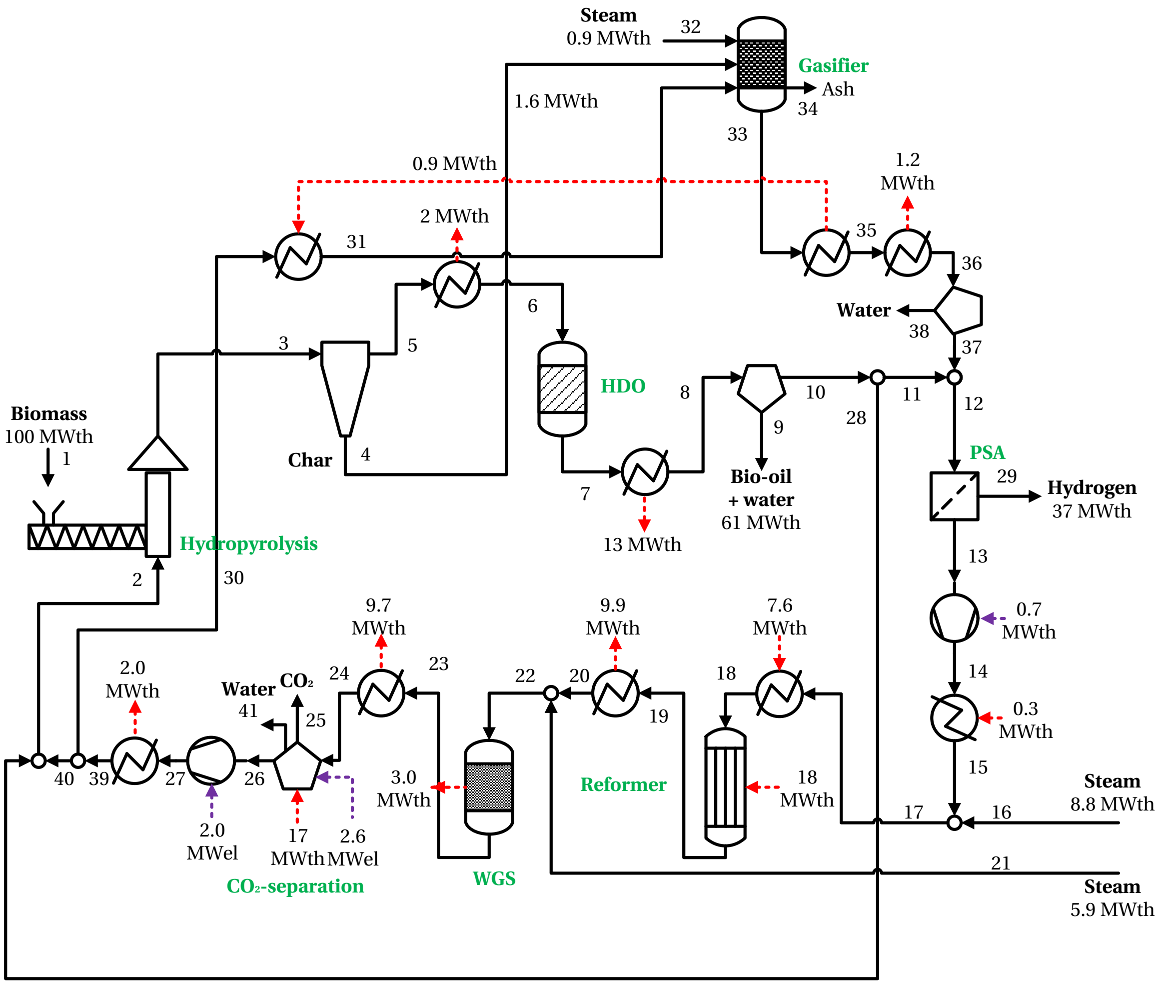

Figure E.13: Process flow diagram of the investigated polygeneration system for production of bio-oil and molecular hydrogen, with chemical absorption.

Table E.9: Process data of the investigated polygeneration system for production of bio-oil and molecular hydrogen, with chemical absorption.

Node	m (kg/s)	T (°C)	p (bar)	Node	m (kg/s)	T (°C)	p (bar)
1	5.76	25	22.4	21	2.17	152	5
2	2.73	25	22.4	22	8.01	223	5
3	8.49	429	22.4	23	8.01	250	5
4	0.52	429	22.4	24	8.01	25	5
5	7.97	429	22.4	25	4.77	25	5
6	7.97	363	22.4	26	1.03	25	5
7	7.97	367	22.4	27	1.03	234	22.4
8	7.97	25	22.4	28	1.84	25	22.4
9 {bio-oil}	1.57	25	22.4	29	0.31	25	22.4
9 {water}	2.22	25	22.4	30	0.13	25	22.4
10	4.18	25	22.4	31	0.13	675	22.4
11	2.34	25	22.4	32	0.24	675	22.4
12	3.03	25	22.4	33	0.79	725	22.4
13	2.71	25	1.1	34	0.1	725	22.4
14	2.71	170	5	35	0.79	394	22.4
15	2.71	219	5	36	0.79	25	22.4
16	3.13	152	5	37	0.7	25	22.4
17	5.84	173	5	38	0.09	25	22.4
18	5.84	750	5	39	1.03	25	22.4
19	5.84	900	5	40	0.9	25	22.4
20	5.84	250	5	41	2.21	25	5

Appendix F. Polygeneration of bio-oil and methanol, with chemical absorption (MeOH-R-G-CA)

The layout of the polygeneration system MeOH-R-G-CA is presented in Figure F.14 with the corresponding data in Table F.10.

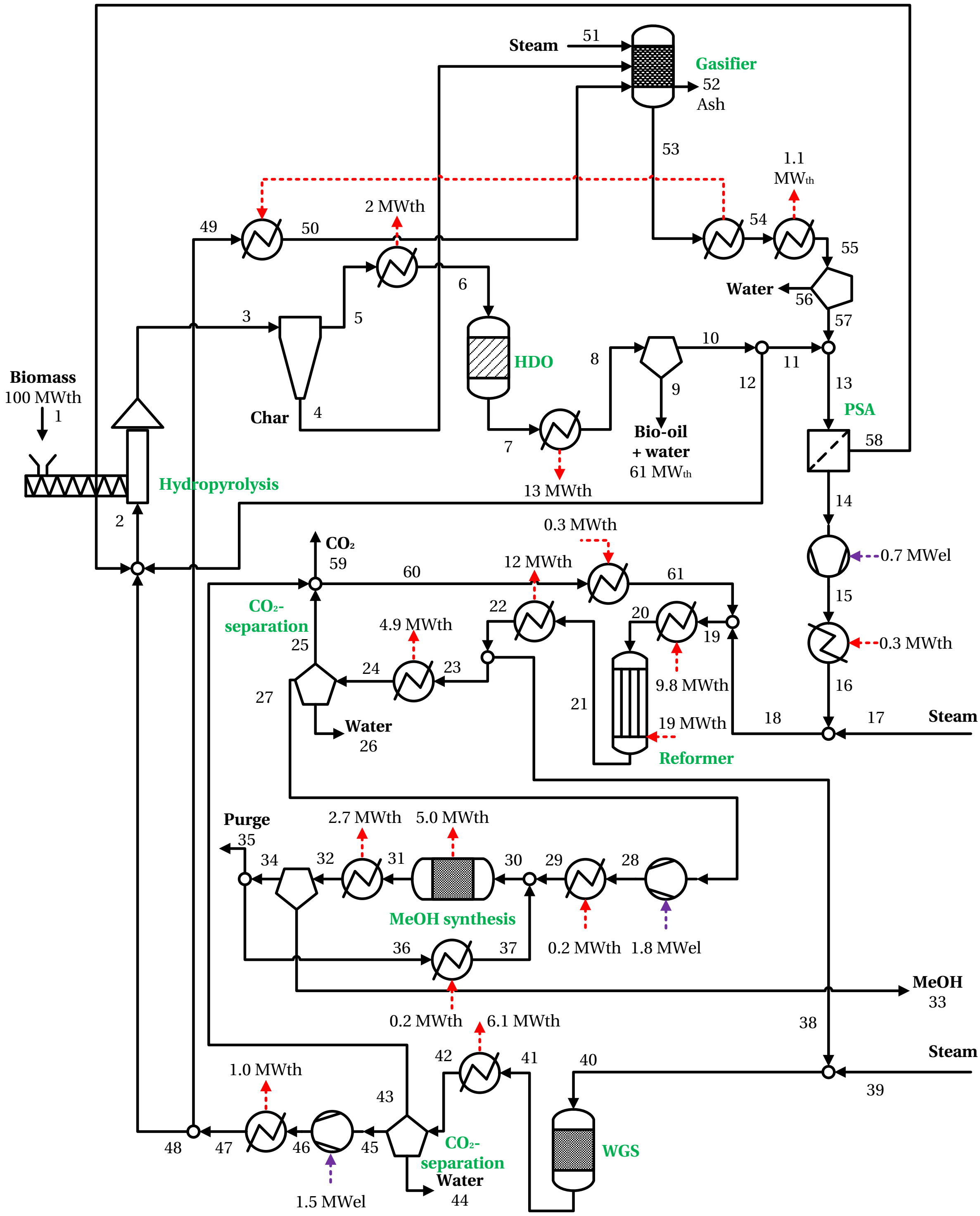

Figure F.14: Process flow diagram of the investigated polygeneration system for production of bio-oil and methanol, with chemical absorption.

Table F.10: Process data of the investigated polygeneration system for production of bio-oil and methanol, with chemical absorption.

Node	m (kg/s)	T (°C)	p (bar)	Node	m (kg/s)	T (°C)	p (bar)
1	5.76	25	22.4	31	2.10	300	96
2	2.38	25	22.4	32	2.10	25	96
3	8.14	429	22.4	33	1.65	25	96
4	0.52	429	22.4	34	0.45	25	96
5	7.62	429	22.4	35	0.02	25	96
6	7.62	363	22.4	36	0.43	25	96
7	7.62	367	22.4	37	0.43	200	96
8	7.62	25	22.4	38	4.63	250	5
9 {bio-oil}	1.57	25	22.4	39	1.55	152	5
9 {water}	2.22	25	22.4	40	6.18	222	5
10	3.83	25	22.4	41	6.18	376	5
11	2.40	25	22.4	42	6.18	25	5
12	1.43	25	22.4	43	3.37	25	5
13	3.15	25	22.4	44	2.05	25	5
14	2.78	25	1.1	45	0.76	25	5
15	2.78	173	5	46	0.76	222	22.4
16	2.78	219	5	47	0.76	25	22.4
17	3.86	152	5	48	0.58	25	22.4
18	6.64	180	5	49	0.18	25	22.4
19	8.49	185	5	50	0.18	675	22.4
20	8.49	750	5	51	0.25	675	22.4
21	8.49	900	5	52	0.1	725	22.4
22	8.49	250	5	53	0.85	725	22.4
23	3.85	250	5	54	0.85	377	22.4
24	3.85	25	5	55	0.85	25	22.4
25	0.99	25	5	56	0.1	25	22.4
26	1.19	25	5	57	0.75	25	22.4
27	1.68	25	5	58	0.37	25	22.4
28	1.68	151	96	59	2.51	25	5
29	1.68	200	96	60	1.85	25	5
30	2.10	200	96	61	1.85	219	5

Appendix G. Polygeneration of bio-oil and methanol, with electrolysis and with chemical absorption (MeOH-E-G-CA)

The layout of the polygeneration system MeOH-E-G-CA is presented in Figure G.15 with the corresponding data in Table G.11.

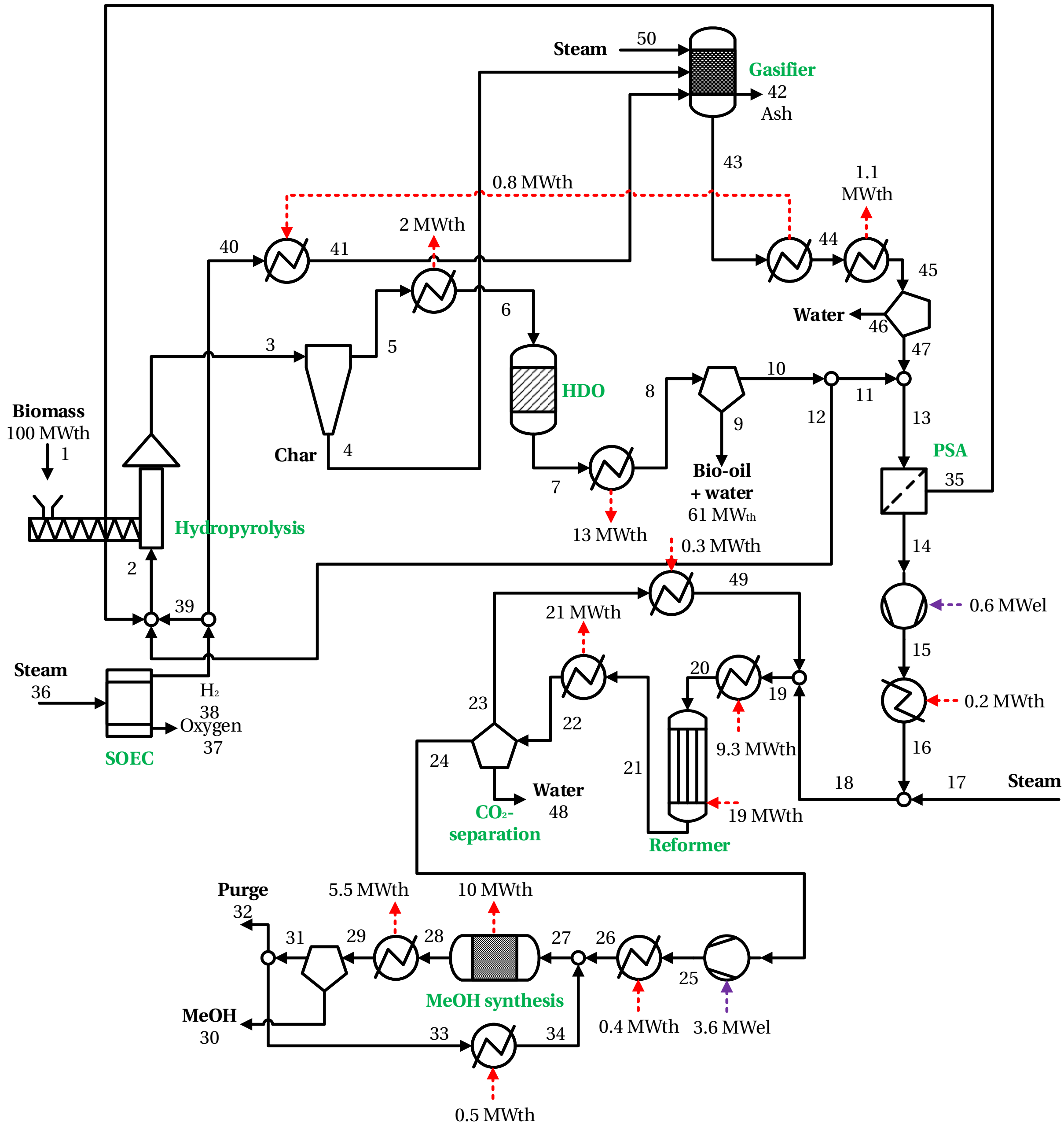

Figure G.15: Process flow diagram of the investigated polygeneration system for production of bio-oil and methanol, with electrolysis and chemical absorption.

Table G.11: Process data of the investigated polygeneration system for production of bio-oil and methanol, with electrolysis and with chemical absorption.

Node	m (kg/s)	T (°C)	p (bar)	Node	m (kg/s)	T (°C)	p (bar)
1	5.76	25	22.4	26	3.48	200	96
2	2.29	25	22.4	27	4.34	200	96
3	8.05	429	22.4	28	4.34	250	96
4	0.52	429	22.4	29	4.34	250	96
5	7.53	429	22.4	30	3.45	25	96
6	7.53	363	22.4	31	0.90	25	96
7	7.53	367	22.4	32	0.03	25	96
8	7.53	25	22.4	33	0.86	25	96
9 {bio-oil}	1.57	25	22.4	34	0.86	200	96
9 {water}	2.22	25	22.4	35	0.32	25	22.4
10	3.74	25	22.4	36	3.15	25	22.4
11	2.03	25	22.4	37	2.80	25	22.4
12	1.71	25	22.4	38	0.35	25	22.4
13	2.68	25	22.4	39	0.26	25	22.4
14	2.36	25	1.1	40	0.09	25	22.4
15	2.36	167	5	41	0.09	675	22.4
16	2.36	219	5	42	0.10	725	22.4
17	3.59	152	5	43	0.75	725	22.4
18	5.95	178	5	44	0.75	384	22.4
19	8.3	176	5	45	0.75	25	22.4
20	8.3	750	5	46	0.09	25	22.4
21	8.3	900	5	47	0.66	25	22.4
22	8.3	250	5	48	2.48	25	5
23	2.34	25	5	49	2.34	178	5
24	3.48	25	5	50	0.24	675	22.4
25	3.48	151	96				

References

[1] Energistyrelsen . The danish climate policy plan - towards a low carbon society. Tech. Rep.; Energistyrelsen; 2013. URL: ens.dk/sites/ens.dk/files/Analyser/danishclimatepolicyplan_uk.pdf.

[2] Baliban RC, Elia JA, Floudas CA, Gurau B, Weingarten MB, Klotz SD. Hardwood biomass to gasoline, diesel, and jet fuel: 1. process synthesis and global optimization of a thermochemical refinery. Energy & Fuels 2013;27(8):4302–24.

[3] Niziolek AM, Onel O, Elia JA, Baliban RC, Xiao X, Floudas CA. Coal and biomass to liquid transportation fuels: process synthesis and global optimization strategies. Industrial & Engineering Chemistry Research 2014;53(44):17002–25.

[4] Onel O, Niziolek AM, Floudas CA. Integrated biomass and fossil fuel systems towards the production of fuels and chemicals: state of the art approaches and future challenges. Current Opinion in Chemical Engineering 2015;9:66–74.

[5] Onay O, Kockar OM. Slow, fast and flash pyrolysis of rapeseed. Renewable energy 2003;28(15):2417–33.

[6] Balagurumurthy B, Oza TS, Bhaskar T, Adhikari DK. Renewable hydrocarbons through biomass hydropyrolysis process: challenges and opportunities. Journal of Material Cycles and Waste Management 2013;15(1):9–15.

[7] Linck M, Felix L, Marker T, Roberts M. Integrated biomass hydropyrolysis and hydrotreating: a brief review. Wiley Interdisciplinary Reviews: Energy and Environment 2014;3(6):575–81.

[8] Resende FL. Recent advances on fast hydropyrolysis of biomass. Catalysis Today 2016;269:148–55.

[9] Dickerson T, Soria J. Catalytic fast pyrolysis: a review. Energies 2013;6(1):514–38.

[10] Venkatakrishnan VK, Degenstein JC, Smeltz AD, Delgass WN, Agrawal R, Ribeiro FH. High-pressure fast-pyrolysis, fast-hydropyrolysis and catalytic hydrodeoxygenation of cellulose: production of liquid fuel from biomass. Green Chemistry 2014;16(2):792–802.

[11] Melligan F, Hayes M, Kwapinski W, Leahy J. Hydro-pyrolysis of biomass and online catalytic vapor upgrading with ni-zsm-5 and ni-mcm-41. Energy & Fuels 2012;26(10):6080–90.

[12] Agrawal R, Agrawal M, Singh N. Process for producing liquid hydrocarbon by pyrolysis of biomass in presence of hydrogen from a carbon-free energy source. 2012.

[13] Marker T, Felix L, Linck M. Hydropyrolysis of biomass for producing high quality fuels. 2013.

[14] Marker TL, Felix LG, Linck MB, Roberts MJ. Integrated hydropyrolysis and hydroconversion (ih2) for the direct production of gasoline and diesel fuels or blending components from biomass, part 1: Proof of principle testing. Environmental Progress & Sustainable Energy 2012;31(2):191–9.

[15] Tan EC, Marker TL, Roberts MJ. Direct production of gasoline and diesel fuels from biomass via integrated hydropyrolysis and hydroconversion processa techno-economic analysis. Environmental Progress & Sustainable Energy 2014;33(2):609–17.

[16] Stummann M, Høj M, Schandel C, Hansen A, Wiwel P, Gabrielsen J, et al. Hydrogen assisted catalytic biomass pyrolysis. effect of temperature and pressure. Biomass and Bioenergy 2018;115:97–107.

[17] Radgen P, Cremer C, Warkentin S, Gerling P, May F, Knopf S. Verfahren zur co2-abscheidung und-speicherung. Studie im Auftrag des Umweltbundesamts UBA, Forschungsbericht 2006;20341110.

[18] Gassner M, Maréchal F. Thermo-economic optimisation of the integration of electrolysis in synthetic natural gas production from wood. Energy 2008;33(2):189–98.

[19] Jensen SH, Larsen PH, Mogensen M. Hydrogen and synthetic fuel production from renewable energy sources. International Journal of Hydrogen Energy 2007;32(15):3253–7.

[20] Laguna-Bercero M. Recent advances in high temperature electrolysis using solid oxide fuel cells: A review. Journal of Power Sources 2012;203:4–16.

[21] Zeng K, Zhang D. Recent progress in alkaline water electrolysis for hydrogen production and applications. Progress in Energy and Combustion Science 2010;36(3):307–26.

[22] Raju AS, Park CS, Norbeck JM. Synthesis gas production using steam hydrogasification and steam reforming. Fuel Processing Technology 2009;90(2):330–6.

[23] Mills GA, Steffgen FW. Catalytic methanation. Catalysis Reviews 1974;8(1):159–210.

[24] Heyne S, Seemann M, Harvey S. Integration study for alternative methanation technologies for the production of synthetic natural gas from gasified biomass. In: 19th International Congress of Chemical and Process Engineering, CHISA 2010 and 7th European Congress of Chemical Engineering, ECCE-7; Prague; Czech Republic; 28 August 2010 through 1 September 2010; vol. 21. 2010, p. 409–14.

[25] Hamelinck CN, Faaij AP. Future prospects for production of methanol and hydrogen from biomass. Journal of Power Sources 2002;111(1):1–22.

[26] Peduzzi E, Tock L, Boissonnet G, Maréchal F. Thermo-economic evaluation and optimization of the thermo-chemical conversion of biomass into methanol. Energy 2013;58:9–16.

[27] Lange JP. Methanol synthesis: a short review of technology improvements. Catalysis Today 2001;64(1):3–8.

[28] Elmegaard B, Houbak N. DNA – A General Energy System Simulation Tool. In: Amundsen J, editor. Proceedings of SIMS 2005 - 46th Conference on Simulation and Modeling. Trondheim, Norway: Tapir Academic Press; 2005, p. 43–52.

[29] Marker T, Roberts M, Linck M, Felix L, Ortiz-Toral P, Wangerow J, et al. Biomass to gasoline and diesel using integrated hydropyrolysis and hydroconversion. Tech. Rep.; Gas Technology Inst., Des Plaines, IL (United States); 2013.

[30] Sircar S, Golden T. Purification of hydrogen by pressure swing adsorption. Separation Science and Technology 2000;35(5):667–87.

[31] Gassner M, Maréchal F. Thermo-economic process model for thermochemical production of synthetic natural gas (sng) from lignocellulosic biomass. Biomass and Bioenergy 2009;33(11):1587–604.

[32] Tock L, Gassner M, Maréchal F. Thermochemical production of liquid fuels from biomass: Thermo-economic modeling, process design and process integration analysis. Biomass and Bioenergy 2010;34(12):1838–54.

[33] Aspen Technology . Aspen Plus – Modelling Petroleum Processes. Burlington, USA: Aspen Technology; 1999.

[34] Chen CC, Song Y. Generalized Electrolyte-NRTL Model for Mixed-Solvent Electrolyte Systems. AIChE Journal 2004;50(8):1928–41.

[35] Soave G. 20 years of Redlich–Kwong equation of state. Fluid Phase Equilibria 1993;82:345–59.

[36] Gross J, Sadowski G. Perturbed-chain SAFT: An equation of state based on a perturbation theory for chain molecules. Industrial & engineering chemistry research 2001;40(4):1244–60.

[37] Higman C. Gasification. In: Combustion Engineering Issues for Solid Fuel Systems. Elsevier; 2008, p. 435.

[38] Gassner M, Maréchal F. Thermo-economic optimisation of the polygeneration of synthetic natural gas (sng), power and heat from lignocellulosic biomass by gasification and methanation. Energy and Environmental Science 2012;5(2):5768–89.